GERHARD VENTER, BE(MECH)

Identification and Manipulation of Lily Bulbs for an Automated Lily Bulb Planting System

Master's Thesis

to achieve the university degree of

Master of Engineering

Master's degree programme funded by: Callaghan Innovations

submitted to

The University of Waikato

Supervisor

Dr. Shen Hin Lim

Waikato Robotics, Automation and Sensing
Head:

Hamilton, June 2019

Affidavit

I declare that I have authored this thesis independently, that I have not used other than the declared sources/resources, and that I have explicitly indicated all material which has been quoted either literally or by content from the sources used.

Date	Signature

Abstract

Automation in agriculture is growing year by year. The goal of automating processes is to provide inexpensive and more effective solutions for everyday problems present in the industry. Automation in agriculture adds value to the product and in turn, to the farmer's infrastructure. This automation also aims to provide higher skill labour for workers that the automation processes substitute. Using machine vision as a means of automating processes is very common in factory environments and is being adapted for the external agriculture environments (i.e. automated detection for produce harvesting).

Machine vision and manipulation techniques for a lily bulb plantation were presented. The techniques were investigated to determine the feasibility of using an autonomous, machine vision based approach to manipulate and plant lily bulbs from a provided source, to pre-augered holes produced by a pre-defined autonomous platform.

The machine vision approach involved taking a top down image of the bulbs and identifying the head positions and what orientation they were facing relative to their root structures. This was achieved using various standard machine vision techniques like segmenting using global thresholding and identification of heads using the Hough circular transform. The investigated manipulation method involved applying the above mentioned vision system to a standard ABB IRB-120 universal manipulator with a three bellow suction gripper to pick up the detected bulbs and manipulate the bulbs in the orientation perceived by the vision system.

It was found that the machine vision algorithm provided a 75 per cent success rate when providing an optimal region of interest within the bulbs head. The success rate is a considerably successful result as the detection algorithm not only needed to detect the location of the bulbs, but the centroid of its head and also determine the approximate orientation relative to each samples individual root structure. The manipulation results showed that the engagement of the suction gripper was a significant component of failure during testing. The observed success rate was at 41 per cent. This high failure rate means that further improvements should be made before a successful end effector and manipulation pair would be achieved. Improving suction rate or developing a specialized gripper for the specific amorphous bulbs would have to be investigated further before there is confirmation of a satisfactory solution for the Automated Lily Planter. Further work could be done to improve the algorithm and fine-tune the output provided. Improvements could be made to optimise the detection algorithm like improved lighting and better contrast between the bulbs colour gradient and that of the platform's background. Further development on the manipulators approach should also be conducted for validation.

Acknowledgements

I would first like to thank my thesis advisor Dr. Shen Hin Lim of the Faculty of Science and Engineering at The University of Waikato. The door to Prof. Lims office was always open whenever I ran into a trouble spot or had a question about my research or writing. He consistently allowed this paper to be my own work, but steered me in the right the direction whenever he thought I needed it.

Author

Gerhard Venter

Contents

List of Figures

1. Introduction

Historically, the concept of 'robot' was introduced to be manufactured biological beings to perform unpleasant manual labour (Hockstein et al., 2007). The advancement of technology in the last century and many defining researches (B. Horn, Klaus, and P. Horn, 1986) (Brooks, 1986) has evolved the definition of robots and autonomous vehicles and now has brought us closer to realise this concept. There's been a few successful applications where autonomous or remote-controlled vehicles has replaced human input to investigate or monitor hazardous environment (Hoefling et al., 2015) (Noguchi et al., 1998) (Günther and Kim, 2005).

The importance of automation in agriculture spans across a wide range of industries. The end goal of automating processes is to provide a cheaper and more effective alternative for common tasks present in industry. This cheaper alternative not only adds value to the farmers yield, but also provides higher quality jobs for the workers previously working on the fields. These jobs involve tasks that require more intellectual labour, rather than the taxing manual labour the workers previously had to endure.

Consistency of operation is another key factor that automation in agriculture adds to industry. A labourer would typically provide inconsistent results in a given task due to factors like fatigue, illness or just a lack of concentration. Automated systems mitigate these factors and it would typically ensure a much more consistent output when it comes to the same task. Whether it be planting, harvesting or packing. An automated robot is expected to provide more consistent results than its manual labourer counterpart. This process consistency provides a more consistent and satisfactory end product for the consumer.

The automation evolution has also affected the perception of farmers and growers in agriculture about automation in recent years. 'Internet of things' is a prime example of a technology being embraced by agriculture industry in sensing and also simple decision making (Ashton et al., 2009). We also see successful harvesting applications (Barnett, 2018) (Rowe, 2015) (McGuinness, 2018).

Lilies by Blewden, as one of the largest producers of lilies in New Zealand, has also embraced the autonomous technology and developed a semi-autonomous vehicle in planting lilies bulb. The current mechanism, as seen in Figure 1.1, automatically drives through a given plantation row within the farm's greenhouse. While it drives through the row, it periodically augers ten holes throughout the width of the row itself. These holes, as seen in Figure 1.2, provide the planting space for the tulip bulbs. After the holes are augered in the ground, two labourers seated on the mechanism manually plant the bulbs in the mentioned holes.

Figure 1.1.: Current System used by *Lilies by Blewden*. The first image provides an overall view of the system, while the second image shows the ten augers used for the process.

Figure 1.2.: Holes systematically augered by the mechanism.

While the vehicle aided a lot of consistency of the holes, manual labour is still required to plant the bulbs and is very challenging to automate the plantation of the lilies bulb. The bulb, as seen in Figure 1.3a, consists of a large head with cloves similar to that of cloves of garlic. The bulb also contains a root structure as well. One of the crucial components of the ABP was that it had to ensure that the root structure would be facing downwards when planted into the augered holes. Since the bulbs would be inserted in a batch process, without knowing its root orientation, the system must ensure that the root faces in the correct orientation before planting.

(a) Sample bulb

(b) Sample crate of bulbs

Figure 1.3.: Sample bulbs and crate used by *Lilies by Blewden*. The crate stores approximately 120 bulbs each

The requirement mentioned would prove to be the most challenging for the detection and manipulation system since the algorithm since it not only needed to detect a relative head centre but also in what orientation it was placed relative to the platform. The current system augurs at an estimated 8 seconds per row, with ten bulbs processed as fast as possible, to ensure that the ABP achieves the unmanned speed required, to keep up with the significant bulb demand, while still providing consistent and accurate results as to where the bulbs are positioned on the platform. From the procedure of lilies bulb planting, it is apparent that the research challenge comes from the bulb identification and the roots direction.

Thesis Objective

This thesis aims to investigate an optimal method to detect the lily bulbs to accurately manipulate the detected bulb into the augered holes. An adequate vision system should be investigated to detect the bulbs position as well as the bulbs relative orientation. Manipulation should be incorporated in such a way to ensure the bulbs be picked up and planted in the right orientation.

Approach

The first step was to investigate existing detection method and also manipulation method. This is followed by fundamentals of machine vision and also the proposed method for detecting lilies bulb with characteristics essential for accurate manipulation. Manipulation method is also covered to investigate the efficiency of the detection method. Investigation into common causes of failure for different stages of manipulation are also investigated and assessed to determine areas of significance when it comes to automatically plant lily bulbs from a given source.

2. Literature Review

The following section provides a review on various algorithms and approaches commonly used in the industry to detect objects from an image that can be applied to lily bulbs detection, also an investigation of end-effector design to manipulate the lily bulb.

2.1. Machine Vision

The use of machine vision to segment objects in a 2-D image has been used commonly in practice. The algorithms used to isolate shapes within an image have been developed throughout the years to be as fast and process as efficient as possible.

The following sub-section provides a brief overview of relevant literature relating to object detection and image segmentation used in industry, as well as conventional techniques used to identify shape characteristics within an image.

Sabanci, Kayabasi, and Toktas, 2016 applied machine vision for classification of wheat grains. This is achieved by utilising Otsu's thresholding method to derive a binary background and foreground region. The algorithm obtains the grains region and computes a simplified, elliptical geometry that resembles the size and shape of the grain as closely as possible. The geometry data provided by the threshold regions get tabulated to classify different wheat genotypes using an artificial neural network as the classifier tool. This article provides useful information as to how a sample image typically gets pre-processed before shape analysis takes place, with the use of global thresholding to segment the foreground samples from the background. after pre-processing, various machine vision techniques could be used more effectively and consistently, be it using a numerical method or with an artificial neural network, which in Sabanci, Kayabasi, and Toktas, 2016, case was the preferred method of investigation.

Sun, 2000 provides a method of detecting topping densities on a pizza using a top down image and processing this image using standard machine vision techniques. Typical algorithms, like thresholding the image and using sobel edge detection proved to be somewhat useful for detection. The results proved to be much more fruitful when splitting the image into localized regions and then conducting segmentation and edge detection on the split images. The end results were very successful, with a segmentation accuracy of over 90 per cent. This method of segmenting using split image shows promise and should be investigated in the lily bulb method as an alternate approach of pre-processing.

Kumar et al., 2014 provides a detailed algorithm to investigate root structures used for a more scientific purpose, to determine a plants genetic makeup via its unique root structure. This research provides a method of detecting the root structure using a sophisticated, pre-trained machine learning algorithm to segment and classifies different critical regions of the roots themselves. Since the tulip bulbs only need to be recognized via its orientation, this highly detailed method of detecting roots might be over complicated for the design specification. The detail required for Kumar et al., 2014 is much higher than the requirement present for the lily bulb detection, since the root structure would only needed to be detected relative to the space provided.

Töreyin et al., 2006 discussed a method of detecting fire hazards present on a video feed using computer vision to detect variations in color gradient, as well as using variations in ordinary motion. The computer vision algorithm aimed to detect fir flickers in a live video feed to ensure a safer environment by providing on-demand fire surveillance. The results proved to be successful. Töreyin et al., 2006 shows that detection using color grading and motion de4tection is a valid method of obtaining information on a video feed and could be considered when investigating a method to detect the lily bulbs.

Mizushima and Lu, 2013 developed a comprehensive solution for optimising the image processing classification of apples, using a support vector machine (SVM), as well as Otsu's method of thresholding. The primary identifier of apple quality in this research was its size. The SVM method is used as a pre-processing method for the apple identifier. It provides a much larger contrast between the background and foreground of the given sample, ensuring a more detailed and precise edge gradient between the apple and the background. Otsu's method provides an automatic global threshold value based on the intensity data provided in a given 1-D image (i.e. grayscale image). After the image had been adequately simplified, a geometric array that was designed to provide a mean diameter of the apple was plotted over the image of the apple. The mean diameter would then be used to classify the quality of the sample.

Mizushima and Lu, 2013 mentioned that Otsu's method does not work adequately if there are variations in brightness and colour on an object, since they may provide spots of data that would be deemed below the calculated threshold. The conclusion presented by Mizushima and Lu, 2013 suggests that the overall SVM method used provided minimal error for multi-channel image segmentation.

Razmjooy, Mousavi, and Soleymani, 2012 discussed using thresholding and defect detection methods to assess the sizes of various potatoes, while also using the defect detection algorithm to classify the potatoes based on quality. The potatoes were initially segmented using Otsu's method of global thresholding to assess the overall size of the sample, then the defects are detected using a color grading system that classifies the potato based on the color gradient presented within the segmented bounds. The results proved to be very successful and shows another example of highly effective global thresholding used for detecting the morphology of a given sample. The potato sample also closely reflects that of the lily bulbs.

Following the past literature on different fruit identification, the following paragraphs cover the standard object identification procedure individually to investigate the possible combination for lily bulb detection processes.

A standard method used for segmenting a single object type from its environment would be to differentiate the target object from its background. Suppose an image contains a dark object with a background with a different colour gradient.

Creating a threshold that would filter all pixels from one set of intensity from another would produce the region of interest required for detecting the target (Gonzalez, Woods, and Eddins, 2003). The proposed vision system would detect a large count discrepancy between the intensity of a given colour-scale. This global threshold would be used to determine the pixels in an image that would be deemed as the object and the pixels that are the background. Figure 2.1 shows the resulting image after a global threshold had been applied to a sample bulb image described at the start of section 2.1. The resulting image would be presented in binary form. Figure 2.1 displays the result processed in MATLAB from the earlier sample image.

It is crucial to test out the output of the threshold on a singular sample, in order to evaluate any inconsistencies present. If there are inconsistencies in one sample, those inconsistencies could be iterated for multiple samples on the same image. The shading seen on Figure 2.1 shows a large region of inaccuracy at the root structure present, due to shading around the roots being detected as a the bulb intensity. This shading could mitigated using adequate overhead lighting that would minimize shading and provide a more detailed root morphology. This shading could provide large detremental effects on the sample, were they more abundant and presented at a lower resolution.

After an edge filter would be applied to a subject, possible regions of interest would be seen mixed with shapes outside of this specified region. Parker, 1996 describe the use of binary erosion and dilation as a method to reduce the information required to represent a specific shape in a binary image.

Figure 2.1.: The sample image of the lily bulb being isolated from its respective background using Otsu's method of global thresholding

In image processing, identifying sudden shifts in information change is crucial in simplifying a model for further analysis. A gradient-based edge detection method would simplify the data for faster processing speeds(Costa and Roberto Marcondes Cesar, 2000b). There are many commonly used edge detection algorithms used in the industry. Conventional techniques were investigated and experimented with a sample bulb image. A gradient-based edge detection algorithm would take an array of a 1-D gradient-based image set (i.e. A grayscale image) and specify any abrupt changes in is shade. The location of these gradient shifts would then be recorded and a much simpler, binary output would be obtained. This output would be useful to plot simplified geometry throughout its geometry, rather than using the original RGB image. Figure 2.2 below shows an RGB sample image taken of a tulip bulb provided by Lilies by Blewden. This image was converted to grayscale and parsed through a Sobel gradient edge detection algorithm on MATLAB. The second image shows the Sobel gradient result, a clear outline of the previous image.

Figure 2.2.: Sample binary image with its edges isolated using a MATLAB sobel edge detection algorithm

It should be noted that a high contrast in the photo taken would increase the overall effectiveness of this method in terms of providing a better-defined result. Also, note how the shadows cast by the bulb interferes with the edge output at the upper root section of the bulb. The interference would be due to the contrast from the shadowed region to the white surface being more apparent than the roots to the shadow. This interference could undermine the final output. It should still be determined whether it would cause a significant error since complex edge identification around the root structure of the bulb is not required for the machine vision algorithm, only a way to discern between it and the bulb heads present on each bulb. After an edge filter would be applied to a subject, possible regions of interest would be seen mixed with shapes outside of this specified region. Parker, 1996 describes the use of binary erosion and dilation as a method to reduce the information required to represent a specific shape in a binary image. A binary image is an array image with only high and low values, instead of the 255 units of gray-scale measurements present on a typical gray-scale image. A binary image provides a simpler input for the binary erosion algorithm as it only needs to discern between the edges of a singular value of measurement.

The Hough transform approximates a line from simplified binary image data. It is instrumental in detecting straight or circular lines for a given pixel set and could prove useful in determining the circular nature of the bulbs head. The current A possible side effect of using the Hough transform would be its processing time required to detect the required object. The detection process typically takes 3-7 seconds on a PC and could hinder the rate at which roots could be planted in a continuous form. The Hough Line Transform also struggles with larger pixel based references, meaning that a large scale image may need rescaling before using a Hough Transform.

2.1.1. Neural Network and Deep Learning

The following sub-section describes an alternate approach to detecting objects in an image, namely using a convolutional neural network (CNN) that had been trained to detect and segment objects within a given RGB image space.

Goodfellow, Bengio, and Courville, 2016 describes deep learning as model designed for a computer to learn from experience and to develop solutions using a hierarchy of different concepts. Deep learning algorithms are proven to be very successful in intuitive problem solving relative to traditional computer aided algorithms. Computer programs were always renowned for being exceptional at processing large amounts of abstract data, but were never exceptional at more vague or intuitive problems. Image classification, for example had always been a challenging problem for computer processes, until deep learning and the use of large convolutional neural networks made image classification a reality on high performance computers.

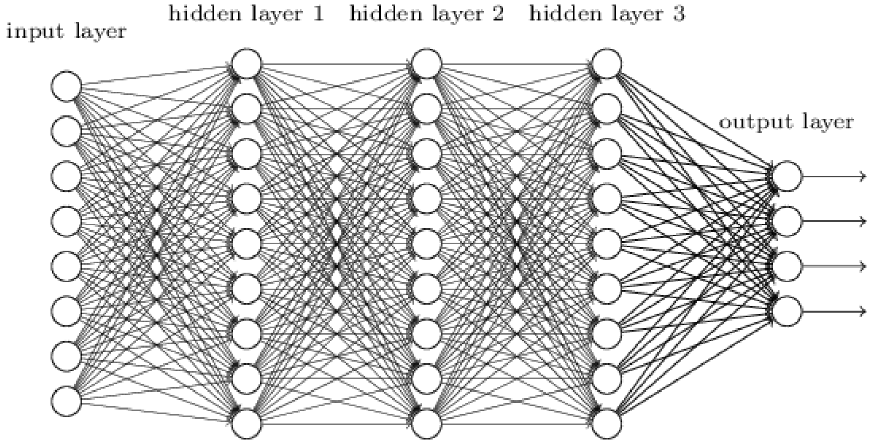

Figure 2.3.: A typical structure of a deep learning algorithm, from Michael Nielsen, 2018. With its dedicated input on the left, with hidden layers of weighted nodes providing an estimated output. These weights had been adjusted to minimize the cost function present at the output during network training

A predefined image classification neural network was used as a base model for detecting the bulb heads from a given overhead image. Various common classification networks (ie. MobilenetV2, Inception) had been evaluated for the specific task of detecting bulb heads and the success rate of identifying the head locations. The mentioned pre-trained networks provide segmentation and classification for a wide array of varying classes, like birds, cars or people. These networks could be retrained to fulfil a specific need. Retraining the model for a new need is called Transfer Learning.

An alternate segmentation method had been conducted using a pre-trained, semantic segmentation convolutional neural network model developed called Deeplab (Chen et al., 2018) (C. Liu et al., 2019). Deeplab provides classification of various common objects as well as semantic segmentation of said objects. Figure 2.4 shows an example of Deeplab semantic segmentation on a provided sample image.

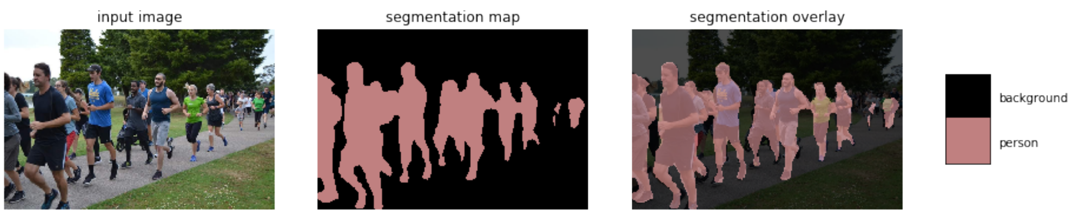

Figure 2.4.: Sample image processed using a Deeplab semantic segmentation using the MobilenetV2 as the main pre-trained network (Sandler et al., 2018). Runners are accurately segmented as people.

2.2. Gripper Investigation

Strategy	Method		Handling ability				Damage type			
			Gripping	Positioning	Orienting	Placing	Bruise	Tear	Break	Deformation
Air	Vacuum	Suction cups	Yes	No	No	Yes	Low	Low	Low	Low
		Pipes	Low	Yes	No	Yes	Yes	Yes	Low	Low
	Pressure	Bernoulli	Yes (no contact)	Low	No	Yes	No	Yes	Low	Low
		Blow	No	Yes	Low	Yes	No	No	Low	No
Contact	Gripper	Electric	Yes	No	Yes	Yes	Low	Low	Low	Low
		Pneumatic	Yes	No	Yes	Yes	Low	Low	Low	Low
		Hydraulic	Yes	No	Yes	Yes	Yes	Low	Yes	Yes
		Rubber	Yes	No	No	Yes	No	Low	No	Low
		Robot hands	Yes	No	Yes	Yes	Low	Low	No	No
	Multibody mechanism		Yes	No	Low	Yes	Low	Low	No	Low
Ingressive	Needles		Yes	No	No	Yes	Yes	No	Yes	No
Fluid	Rheological change		Yes	No	Low	Yes	Low	Low	No	Yes
Product properties	Gravity		No	Yes	Low	Yes	Yes	Low	Yes	Yes
	Piling up, pushing		No	Yes	Low	Yes	Yes	Low	Low	Yes
	Dynamic		No	Yes	Low	Yes	Yes	Low	Yes	Yes
	Scooping up		No	Yes	Low	Yes	Low	Yes	No	No
	Vibration		No	Yes	Low	Yes	Yes	Yes	No	No

Figure 2.5.: Table of various gripper technologies extracted from Blanes et al., 2011

End effectors are devices at the end of a given manipulator, designed in a way that interacts with a given subject in a specified manner. A manipulator without an adequate end effector for the problem would be useless under the application. The following section delves deeper into different end effector designs and provides various examples of common end effectors used for similar design criteria required for the automated bulb planter. Blanes et al., 2011 provides a review on various gripper designs for fruits and vegetables used in factory designs. The review provides a detailed comparison of various manipulation designs, as seen in Figure 2.5. The three main designs considered in this review are the vacuum, contact and ingressive methods.

Hayashi et al., 2011 used a suction cup with a 4DOF arm to adequately pick up and orient strawberries with the end caps facing upwards, for packaging purposes. A camera detects the end cap orientation for the given strawberry. The arm would then rotate and align itself to the strawberry end cap, use the suction cup to pick lift it at an angle and places the strawberry at the required packaging area. The following Figure 2.6, extracted from Hayashi et al., 2011, shows the cups angle of approach during the lifting stage. The suction gripper technique would prove useful for the Automated Bulb Planter since it would not only be able to orient the bulb adequately, but the arm could also be used to plant it from the suction cup straight to the provided auger holes. One main issue with suction cups would be its tendency to underperform in porous environments. One of the main problems facing a suction cup design for the tulip bulb application would mainly be the large continuous energy consumption required for consistent use. The estimated power consumption needed for a single suction cup would be around 1 Kilowatt, based on the strawberry cups required usage.

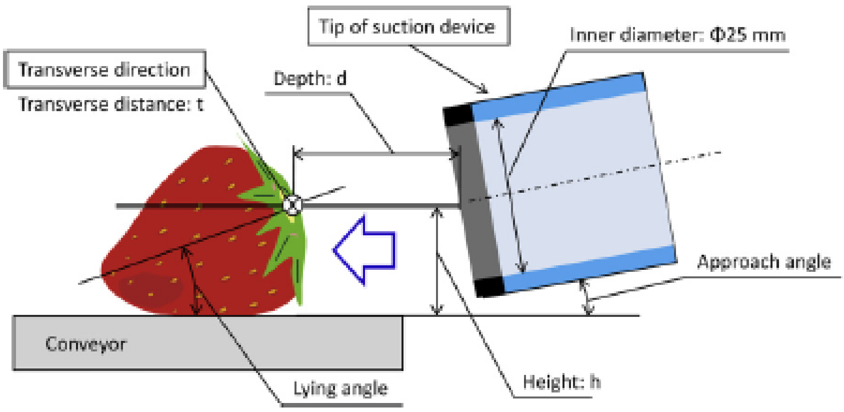

Figure 2.6.: Sample gripping method. Image extracted from Hayashi et al., 2011.

Another essential requirement, according to Blanes et al., 2011, would be a relatively clean contact surface for the cup to operate accordingly. This is not feasible for the tulip bulbs since they are initially stored in soft grit and are not thoroughly cleaned before planting. The suction gripping shows promise and could provide a solution for the bulb manipulation problem. A prototype of the concept would be conducted to investigate the aforementioned potential issues with the design, specifically relating to its consistency upon picking up a sample and how a commercial cup would handle peat and a dirty sample.

Another adaptation method for a vacuum based design was also investigated. Han et al., 2018 provides a design investigation revolving around a universal gripper for different shapes. It uses a flexible holder filled with granular material as its gripper. Upon contact, the gripper wraps around the object, and a vacuum is applied within the flexible bag to provide a shaped gripper for the given object. The design uses a combination of suction and friction to lift any given shaped object within a range of sizes relative to the end effectors diameter. The granular gripper could provide another solution to the amorphous contact surface required during picking. The consistency of the design should be investigated, and the material used for the wrapping of the grains should be carefully considered since, after multiple uses, the membrane could tear and break the gripper. Another issue would be the normal force required to pick up the bulb since the main benefit of a suction-based design would be its ease of angular approach due to it not requiring any normal force for lifting.

Foglia Mario and Reina, 2006 provides a method of harvesting radicchio plants using a large gripper tool to harvest the produce by physically pulling it from the earth. It uses a threshold based computer vision tool to identify the centroids of the samples and maps the motion required by the arm in order to direct it and harvest the targeted radicchio. The use of contact grippers could provide multiple disadvantages that could prove the manipulation method undesirable for the given use. The speed at which the grippers pick up and manipulate a given sample could be too slow as it must first identify a location of attack for the grippers, pick the sample up, rotate and drop the sample all in one for one given cycle. Since the bulb planter plants ten bulbs every 20 seconds, the rate at which the gripper manipulates a sample would take too long.

2.2.1. Summary

In summary, this section covers literature review on machine vision, different types of end-effector grippers for manipulation, and also the potential of neural network to be applied as part of the object detection. This literature review showed a few different techniques that can be useful for developing the new lily bulb technique and also provided the important characteristics of lily bulb such as centroid and root tip direction. Different effectors were also investigated to ensure that the lily bulb is not damaged and can be transitioned to the auger holes. The complexity of the lily bulb shapes, in particular the root section, can also be aided by neural network application.

3. Machine Vision for Lily Bulb Detection

The requirements of the machine vision system are two-fold. Firstly to identify the head positions of all the bulbs present on the platform at a given time, and secondly to provide an adequate estimate of the relative orientation of each head detected, being either north or south facing.

The vision system must also produce an accurate centroid for the head of all the bulbs present on the platform. The centroid should be within the bounds of the bulb head, for optimal suction contact and gripping. The following chapter will discuss the two main machine vision varieties tested to detect the bulb orientation and head locations for the required application of manipulating and planting the bulbs to an augured hole.

3.1. Methodology

The techniques used for the numerical method were derived from (Gonzalez and Woods, 2001), (Gonzalez, Woods, and Eddins, 2003), (Costa and Roberto Marcondes Cesar, 2000a), (Parker, 1996) and (Solomon and Breckon, 2011). Figure 3.1 provides a flow diagram that describes the steps taken to provide an adequate numerical algorithm for detecting the bulb heads and their orientation. Further detail into each component of the algorithm will be discussed. The following section describes the step by step approach described in Figure 3.1 and provides sample images of each individual process using Figure 3.2 as the example image.

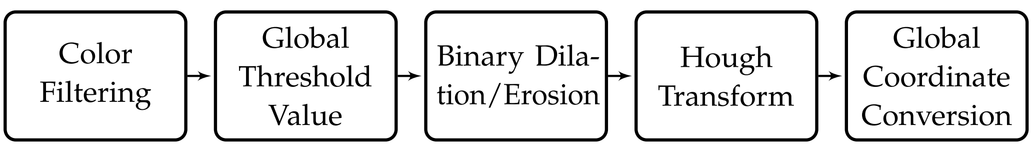

Figure 3.1.: A process flow of the tested numerical algorithm used for bulb detection and orientation identification

The original image taken by the camera consists of an RGB image of all bulbs present within the length of the platform. The blue gradient of the original

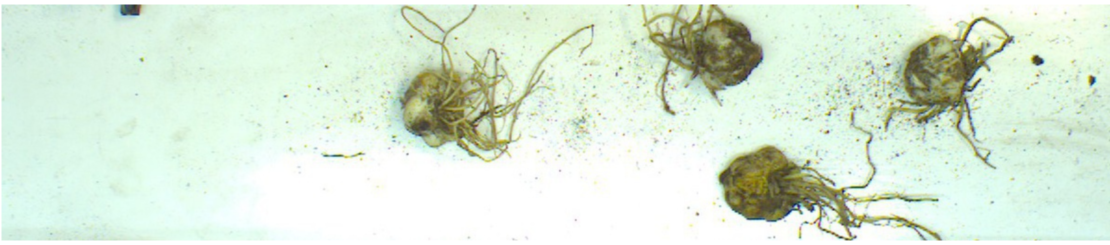

Figure 3.2.: Sample image used to provide context on the approach used during for the numerical detection method.

image gets isolated since it is the gradient with the most substantial contrast between the bulb foreground and the current white background. The blue filter had been confirmed after numerous testing to be the best gradient for threshold segmentation between the bulb foreground and the white background of the conveyor belt used for manipulation testing. Figure 3.3 provides the sample image with only the blue gradient present.

The assumption of using a blue gradient filter presumes that the majority of the bulbs have a similar color gradient throughout testing.

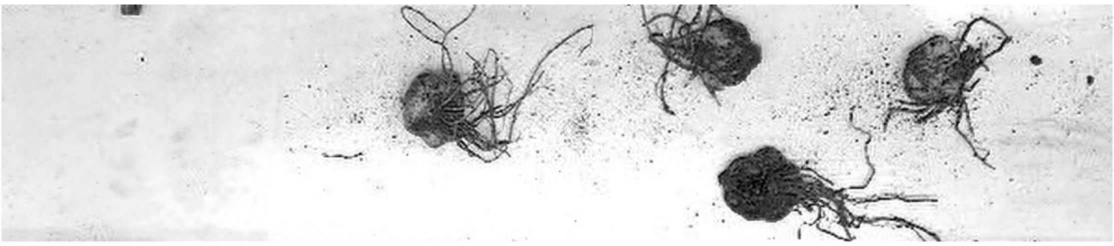

Figure 3.3.: The initial sample image with the blue gradient isolated within the sampled RGB image.

A Gaussian filter had been applied to the blue-filtered image to reduce the noise present in the sample image by blurring the sample image. It should also be noted that increasing the blur to a significant degree would significantly reduce detail present in the image and may provide a misrepresentation of the bulbs morphological shape.

The following two-dimensional Gaussian distribution equation had been applied to the image.

$$G(x, y) = \frac{1}{2\pi\sigma^2} e^{-\frac{x^2+y^2}{2\sigma^2}} \tag{3.1}$$

where σ is the standard deviation of the given pixel intensity distribution.

The output kernel provides a mean bell-shaped curve over a given discrete amount of pixels. The kernel size had been adapted to fulfil the function, with the final iteration using a kernel size of 11 pixels squared. Figure 3.4 shows the output image after a Gaussian filter had been applied with a kernel size of 11 pixels.

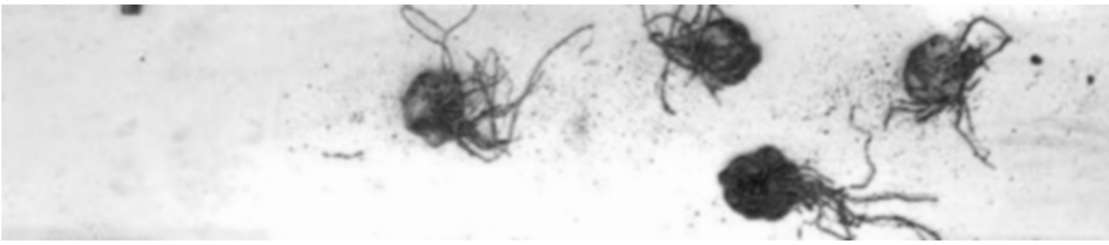

Figure 3.4.: The blue filtered image after a Gaussian filter had been applied to reduce noise

Otsu's method for global thresholding was used to segment the image into two components, namely the pixels that relate to the background and the pixels that relate to the foreground, which in the case of the sample, was the bulbs with their respective heads and root structures.

Figure 3.5.: Otsu's global threshold method used on the blue filtered sample image displayed in Figure 3.3

A global threshold value is determined using Otsu's method that would discern between the foreground and background pixel intensities. Otsu's method uses a grayscale images pixel intensity distribution and finds the threshold pixel intensity value that would maximize the inter-class variance within the given distribution between the two classes present, namely the bulb intensity and the background intensity.

Otsu, 1979 provides the weighted inter-class variance function applied to the provided intensity distribution on a given image. k represents the threshold value and should be adjusted so that $\sigma_B^2(k)$, the inter-class variance is maximized.

$$\sigma_B^2(k) = \frac{[\mu_T \omega(k) - \mu(k)]^2}{\omega(k)[1 - \omega(k)]} \tag{3.2}$$

where

$$\omega(k) = \sum_{i=1}^{k} p_i \tag{3.3}$$

and

$$\mu(k) = \sum_{i=1}^{k} i p_i \tag{3.4}$$

p_i states the pixel fraction at a given gray level i:

$$p_i = \frac{n_i}{N} \tag{3.5}$$

n_i is the pixel count at gray level i and N being the total number of pixels present on the image. μ_t defines the total mean level:

$$\mu_t = \mu(L) \tag{3.6}$$

L is the maximimum gray level value present in the sample.

Otsu's method assumes a substantial variation between the foreground pixel intensity and the background pixel intensity to determine an intensity threshold value that would discern between the intensity of the bulbs from the belts white colour. The resulting output would be a binary image displaying the segmented bulbs from its background. Figure 3.5 shows the output of the head of bulbs present, with some remnants of peat or other darker objects that were detected to be higher than the set threshold value.

Figure 3.6 defines the sample images pixel distribution. The vertical line was the predicted Otsu threshold value, separating the expected foreground and background pixel clusters.

The output provided after global thresholding, is a binary image with a background class and bulb class visible on the two-dimensional image. This binary image would be dilated slightly to account for any patches of isolated pixels the threshold deems too low intensity on the head of the bulb itself. After the initial dilation, the image then gets eroded to the extent that all of the root structures have been removed from the image and only the centre of the head of each bulb remains. This erosion also removes any considerable amounts of peat present on the platform as well. The remaining head centres would be used to determine the region of interest for manipulation.

Binary erosion is a method of reducing external information on the edges of a given binary image. A small binary matrix (i.e. a 4x4 matrix compared to the 1000x1200 image) gets superimposed for each pixel present on the original binary image. Every time the matrix superimposes a pixel, it checks if it correlates with the matrix surrounding the mentioned pixel. If they correlate, then the pixel becomes a 1, and the pixel would be 0 if they do not correlate.

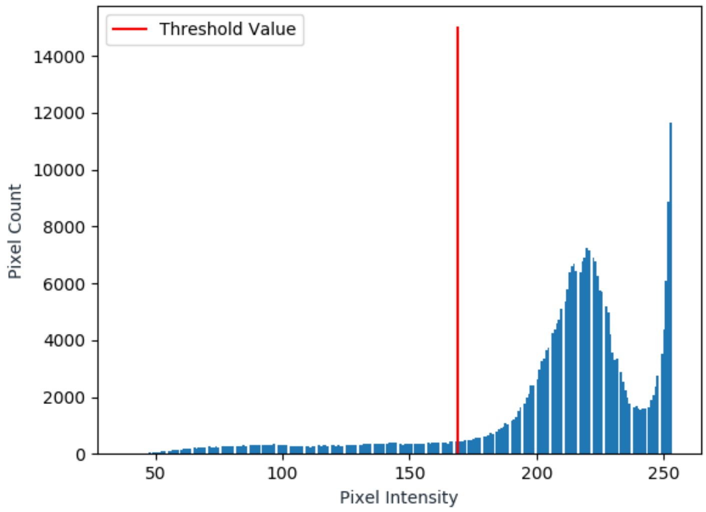

Figure 3.6.: Pixel distribution of the blue gradient of the sample image after a gaussian filter had been applied. The Otsu threshold value can be seen with the vertical line separating the predicted foreground and background pixels.

Figure 3.7.: Eroded binary image with only the bulb heads present, with some remnants of their respective stem structures.

$$\begin{bmatrix} 1 & 1 & 1 \\ 1 & 1 & 1 \\ 1 & 1 & 1 \end{bmatrix} \begin{bmatrix} 1 & 1 & 1 & 1 & 1 & 1 & 1 & 1 & 1 & 1 \\ 1 & 1 & 1 & 1 & 1 & 1 & 1 & 1 & 1 & 1 \\ 1 & 1 & 1 & 0 & 1 & 1 & 1 & 1 & 1 & 1 \\ 1 & 1 & 1 & 1 & 1 & 1 & 1 & 1 & 1 & 1 \\ 1 & 1 & 1 & 1 & 1 & 1 & 0 & 1 & 1 & 1 \\ 1 & 1 & 1 & 1 & 1 & 1 & 1 & 1 & 1 & 1 \\ 1 & 1 & 0 & 1 & 1 & 1 & 1 & 1 & 1 & 1 \\ 1 & 1 & 1 & 1 & 1 & 1 & 1 & 1 & 1 & 1 \\ 1 & 1 & 1 & 1 & 1 & 1 & 1 & 1 & 1 & 1 \\ 1 & 0 & 1 & 1 & 1 & 1 & 1 & 1 & 1 & 1 \end{bmatrix} \begin{bmatrix} 0 & 0 & 0 & 0 & 0 & 0 & 0 & 0 & 0 & 0 \\ 0 & 1 & 0 & 0 & 0 & 1 & 1 & 1 & 1 & 0 \\ 0 & 1 & 0 & 0 & 0 & 1 & 1 & 1 & 1 & 0 \\ 0 & 1 & 0 & 0 & 0 & 0 & 0 & 0 & 1 & 0 \\ 0 & 1 & 1 & 1 & 1 & 0 & 0 & 0 & 1 & 0 \\ 0 & 0 & 0 & 0 & 1 & 0 & 0 & 0 & 1 & 0 \\ 0 & 0 & 0 & 0 & 1 & 1 & 1 & 1 & 1 & 0 \\ 0 & 0 & 0 & 0 & 1 & 1 & 1 & 1 & 1 & 0 \\ 0 & 0 & 0 & 1 & 1 & 1 & 1 & 1 & 1 & 0 \\ 0 & 0 & 0 & 0 & 0 & 0 & 0 & 0 & 0 & 0 \end{bmatrix}$$

Figure 3.8.: An example of binary erosion on a sample matrix. The left, 3x3 matrix defines the erosion matrix used to superimpose on the second matrix, which is a sample 10x10 matrix with some discontinuities represented by the zeroes present. The third matrix represents the output after erosion had occurred throughout the sample matrix.

Figure 3.8 describes an example situation with a 3x3 erosion matrix. the initial 20x20 matrix gets eroded based on that 3x3 matrix.

Binary dilation uses the same principle as binary erosion, but instead of removing the edges, it expands these edges. It acts like binary erosion but is its matrix is inverted.

Since the erosion magnitude value used to erode and dilate the threshold image remains constant throughout samples, it is assumed that the sample bulbs do not vary significantly in size throughout all tests. If a significantly large bulb is tested, then the root structure present may not have been entirely eroded, while if the sample is significantly small then the samples head structure may get its shape completely deformed and would prove to be difficult to detect its shape characteristics in future detection processes.

A circular Hough transform provides the coordinates for the centroids of circular structures with the highest likelihood to be displayed on the eroded image. The circular Hough transform is used instead of a centre of area calculation because the eroded heads visible in Figure 3.1 could still provide some detail of the stem of the root structure if the bulbs root structure were prominent enough. The set of centroid data would be transferred to the manipulator for lifting and planting.

$$\rho = x * cos(\theta) + y * sin(\theta) \tag{3.7}$$

where ρ defines the shortest distance between the origin and the line and θ the angle from the horizontal axis to the line connecting the origin with the shortest distance to the line.

The defined line gets superimposed over a binary image and the count of pixels Q that correlate to the line gets recorded for the specific input values for ρ and θ. This is done for a finite amount of lines, with the highest Q values determining the highest likelihood of a line being present at the correlating parametric values.

The Hough transform for a circle would use a similar approach, but instead of using the parametric equation of a line to determine the shape to look for, it would instead use the parametric equation of a circle.

$$r^2 = (x - x_0)^2 + (y - y_0)^2 \tag{3.8}$$

where r is the radius, and (x_0, y_0) being the circles centroid relative to the origin.

Similar to the Hough line transform, the circular transform finds the pixel count Q for the image superimposed by the given circular function for finite cases of r, x_0 and y_0, With the largest values of Q representing the highest likelihood of a circular shape being present at the corresponding parameters.

After the centroids had been discovered, the coordinates get overlapped to the original binary image and compared to the overall bounds of each segmented object. The numerical method assumes that the bulb would be facing in an orientation where the bulb heads are position offset from the centroid of the Rectangular region of interest since the root structure provides a broad spread of each bulbs region of interest. Figure 3.9 provides the output of the overall numerical method. Each centroid and orientation value pair would be sent to the respective manipulator for the planting phase of the process.

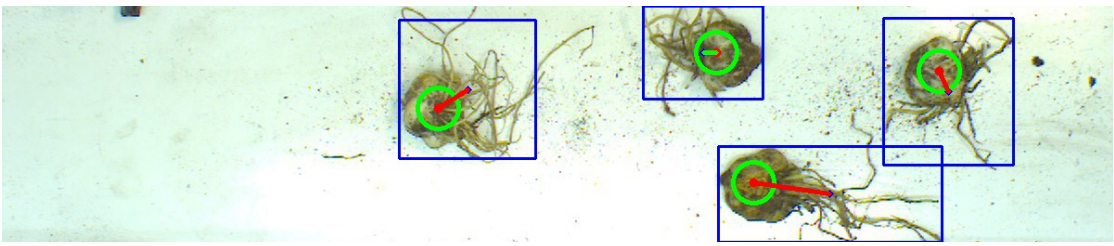

Figure 3.9.: The output of the numerical algorithm. The circles represent the Hough transform estimate of the centre of each bulb head based on the eroded binary image shown in Figure 3.7. The rectangles represent the ROI of each individual bulb and the arrowheads depict the relative orientation of eahc bulb.

3.1.1. Global Coordinate Conversion

The relative image coordinates of the head position and their relative orientation (being either left or right facing) gets converted to a global linear coordinate framework that the manipulator could use to position itself to the heads of the bulbs. The transfer to a linear coordinate frame was done using a linear transfer function relating between the relative pixel distance and the linear distance the arm travels on its encoder.

The transfer function had been constructed based on the equations:

$$x_d = x_{im} * M + x_0 \tag{3.9}$$

$$y_d = y_{im} * M + y_0 \tag{3.10}$$

where (x_d, y_d) is the coordinate value for the target relative to the manipulators origin, in mm. (x_{im}, y_{im}) is the pixel coordinate data relative to images origin, in pixel count.(x_0, y_0) the offset between the image origin and manipulators origin, in mm.

M is the metric distance to pixel ratio present in the image, in mm/count. M is measured using the following relationship:

$$M = \frac{mag[(x_{d1}, y_{d1})(x_{d2}, y_{d2})]}{mag[(x_{im1}, y_{im1})(x_{im2}, y_{im2})]} \tag{3.11}$$

where $mag[(x_{d1}, y_{d1})(x_{d2}, y_{d2})]$ is the magnitude between two known points relative the manipulators point of origin in mm and $mag[(x_{im1}, y_{im1})(x_{im2}, y_{im2})]$ is the magnitude between the same two points measured relative to the images origin, in pixel count.

The linear transfer function provided metric coordinate data that the ABB manipulator could use to approach the predicted target using the suction cup manipulator.

3.2. Evaluating Success

A successful vision system for this experiment would be able to detect the centre of the head as closely as possible for the manipulator to approach and lift the detected bulbs successfully. An experiment had been conducted to evaluate the optimal algorithm for the manipulation of the bulbs.

Figure 3.10 shows three successfully detected bulb sets using the numerical method mentioned in section 3.1. the line drawn between the centroid of the bulb heads and the centroids of their region of interest depicts the expected orientation for the tested bulb.

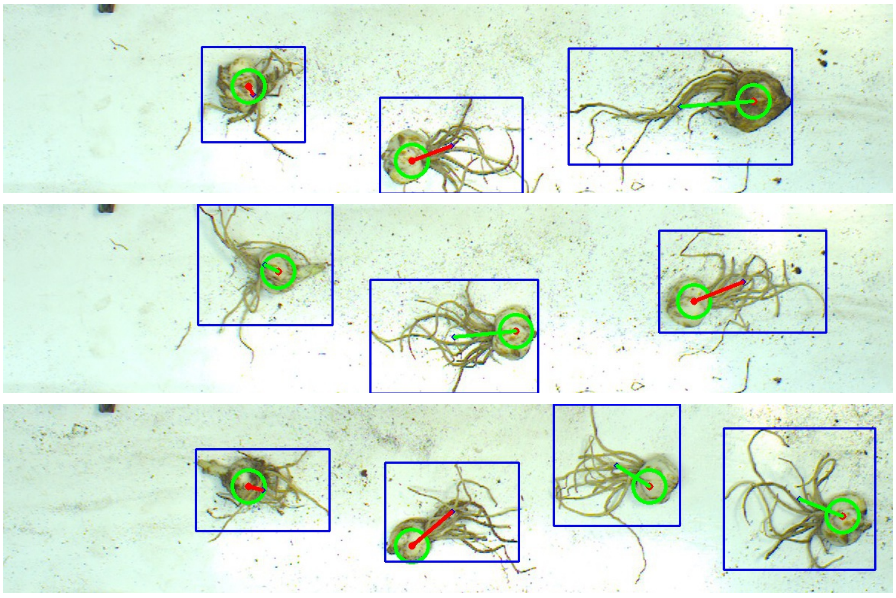

Figure 3.10.: Examples of successfully detected bulbs, The red centroid displays the calculated centroids, while the blue box describes each bulbs bounding region. the line between the centroid of the head and the centroid of the bounding box indicate the expected orientation for each bulb

3.3. Results

3.3.1. Experimental Setup

The following section describes a brief instruction to the setup method used for obtaining the images of the bulbs for both methods. Both methods use the same testing images so the setup would apply for both cases. The process flow chart, as seen in Figure 3.11, provides a brief description of the required steps for testing.

Bulbs are placed linearly with roots parallel to the linear direction, either front facing or rear facing. This binary orientation would be adequate since it was proven that the bulbs could be manipulated mechanically on the belt using

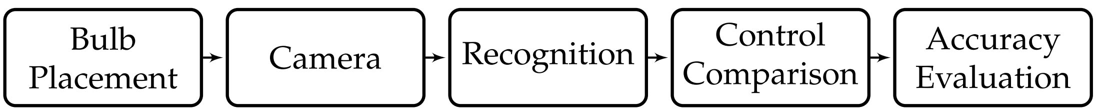

Figure 3.11.: Process Flow of the experimental setup required for a successful detection analysis

a ramp feed that would either face the bulbs on one direction or the on the opposite direction. Figure 3.15 shows an example of the bulbs being placed on the platform, spaced and placed in either a left or right facing direction. Figure 3.12 shows the overall final assembly used for testing.

A camera placed 1.1m above the bulbs ground plane, takes an image of the bulbs, as seen in Figure 3.13a. The camera would be taking a top facing image that would encompass the majority of the belt, and the detectable area would also be the possible area of manipulation for the manipulator. Figure 3.14 provides an example image taken of the entire scope of the camera. The image gets cropped to the proper region of interest as seen in Figure 3.15.

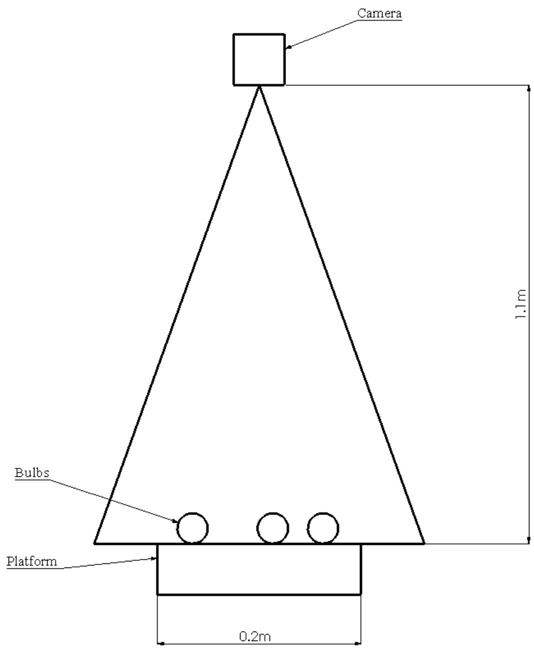

Figure 3.12.: A diagram representing the setup used for the machine vision system used for testing. The camera is positioned centrally 1.1m above a given platform, taking images of the sample bulbs provided by *Lilies by Blewden*

The image is processed using the numerical or neural network method to determine the relative location of all the bulb heads displayed, as well as their respective orientation.

3.3.2. Head Detection

Before presenting the detection results of the machine vision algorithm, a successful detection occurrence should be defined and assessed. Where, within the bulbs head-region, is a good region of engagement for the manipulator to grip the bulb samples.

(a) Testing Platform

(b) Camera used for image capture

Figure 3.13.: The overall setup used for experimental testing. The camera detects from a height of 1.1m identifies a range of 800mm in length along the whole width of the belt of 200mm.

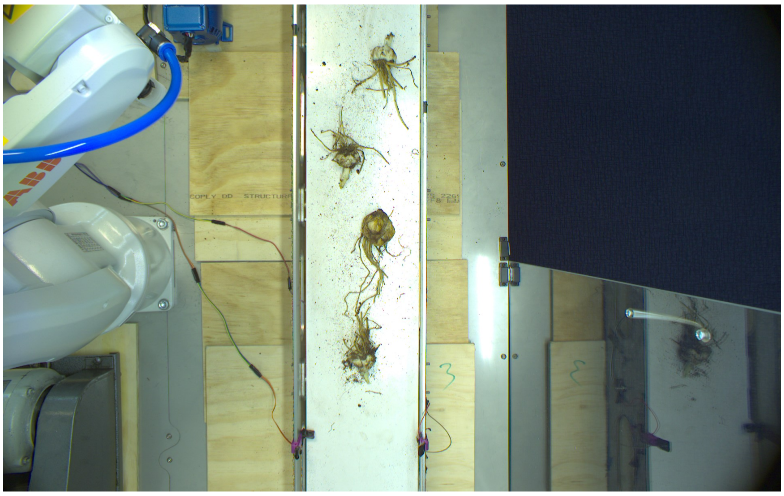

Figure 3.14.: Sample image if the camera taking a top view image of the platform

Figure 3.15.: Cropped and rotated image of the sample image present in Figure 3.14

Testing had been conducted to evaluate the best regions of engagement for the gripper to engage and manipulate the tested bulb heads provided by Lilies by Blewden.

The test manipulator (ABB IRB-120) had been manually placed within a given region of the centroid of the bulb heads used for testing. Three regions were evaluated, namely when the manipulator end-effector engaged close to the bulb heads centroid (within 5mm of the heads perceived centroid), when the end effector engaged within a 5mm to 15mm radius of the bulbs perceived centroid and then tested at edge cases where the end effector engaged it between 15 to 20mm outside the centroid of the bulb head. The bulb heads typically range from 15mm to 30mm in radius, so the final region would sometimes completely miss the sample entirely, given a small enough sample.

The only manual component of the test was to position the manipulator for engagement, the actual engagement and manipulation process was standardized using an automated script that would engage and manipulate the bulb head at a constant speed. The end effector used was a three bellow suction cup that would suck at contact.

Table 3.1 represents a set of successful and unsuccessful manipulation manually attempted by the ABB IRB-120 robotic arm. The attempts were cross-referenced with three gripper engagement regions. Figure 3.16 shows the three regions in question, namely within 5mm of the perceived centroid of the bulb, between 5mm to 10 from the centroid, and the edge cases where the cups centroid was perceived to be close to the edge of the bulb head, between 15 and 20mm from the centroid.

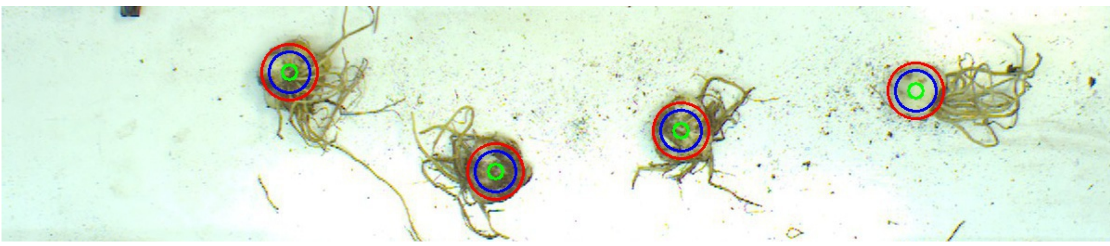

Figure 3.16.: Regions mentioned for success evaluation. The Red circle represents the 20mm radius, Blue the 15mm radius region and the green region is within 5mm of the perceived centroid.

The results indicate a high level of success within the 10mm region. This success rate implies that any detected regions within 10mm from the centroid were seen as valid targets for manipulation.

The set of test images (>100 images) were evaluated, and the relative head centres and orientations labelled manually. Both vision systems were tested based on the manually selected set of bulb coordinates and the overall accuracy of the two methods were compared.

Region	Distance from Centroid (mm)	Success Rate (Percentage)
Close	<5	84.62
Within Head	5 - 15	80.77
Edge Case	15 - 20	38.46

Table 3.1.: Success rates relative to the perceived engagement region. The results from the investigation would provide validation for a successful region of detection within for the machine vision algorithm.

The results from the manual engagement region evaluation show a significant variation (from 80.77 per cent to 38.46 per cent) in successful engagement from Region 2 (Within Head) and Region 3 (Edge case). The majority of these extra failures were due to the suction gripper not fully enveloping the sample during contact. These failures indicate that the majority of successful gripper engagements took place within 15mm relative to the bulbs centroid. It would be safe to assume a successful target for the machine vision algorithm is anywhere within 15mm from the actual centroid of the bulb itself. This 15mm assumption would be used to evaluate the performance of the machine vision algorithm in future discussions.

As seen in Table 3.2 for 74.26 per cent of the recorded cases, a result was calculated within the radius of the smallest possible bulb size present at *Lilies by Blewden*, of around 15mm in radius. A 59 per cent success rate was present within a 10mm radius of the expected centroid. Data for each case can be found in Appendix B.

Figure 3.17 provides the normal distribution of all the calculated bulb positions against the relative accuracy of each individual case.

Radius From Centroid (mm)	Successful Targets (Percentage)
5	19.12
10	59.56
15	**74.26**
20	77.94
25	78.68

Table 3.2.: Variation between the success rate of the numerical method compared to the radius from the predicted centroid

A 75 per cent success rate is a considerably successful result as the detection algorithm not only needed to detect the location of the bulbs, but the centroid of its head and also determine the approximate orientation relative to each samples individual root structure. Iteration would also be incorporated during the manipulation phase of the process. This incorporation means that if failure did occur during detection and manipulation, the manipulator would conduct another opportunity since the bulb is still present on the platform itself.

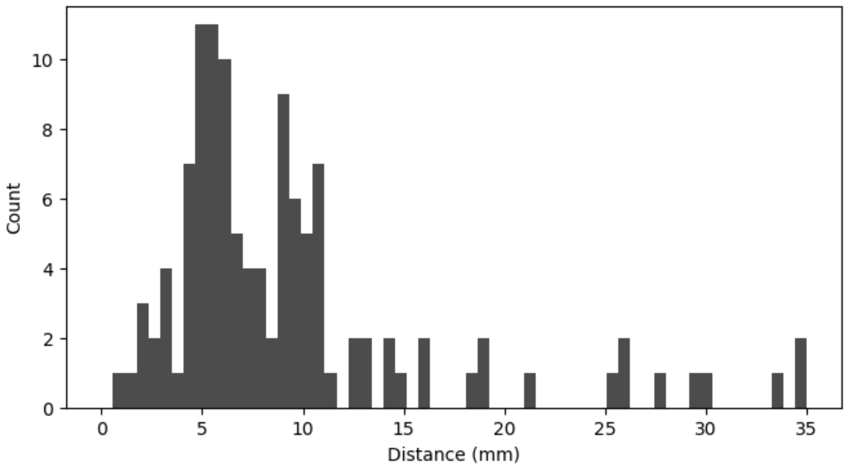

Figure 3.17.: Distribution of the distances between the predicted bulb centroids against the centroids calculated by the numerical algorithm

3.3.3. Observations

The shape analysis algorithm was found to be consistent in detecting either the small white oriental bulbs as well as the larger, traditional bulb types used by *Lilies by Blewden*. This implies that the algorithm detects varying bulb sizes relatively consistently and can be used for both cases.

A typical issue observed in the results was that some of the bulbs had regions within the bulb seen as the same gradient as the background of the image, as seen in a threshold example in Figure 3.18. The incorrect gradient detection provides inconsistent shape analysis since the threshold value commonly excludes glossy areas of the oriental bulb heads. This can be mitigated with a belt colour that is contrasting to any of the bulbs used in the tests and should be considered in future testing.

Figure 3.18.: Sample image depicting the issue with otsus threshold present in some of the test samples. The rightmost bulb has a cavity present that would propagate with further erosion, deteriorating its shape characteristics.

The Hough circular transform provided inconsistent results and required tweaking for edge cases. This tweaking makes sense since there are inconsistencies in the shape and size of the bulbs themselves that would provide these inconsistencies during detection. If a bulb with a smaller than average head and a larger than average root structure is present, the detection algorithm may represent a significant component of the root structure as part of the head itself, since erosion value remains constant. The constant erosion value would mean that if the heads are of a similar size and shape, which could be categorized by the bulb varieties present, then the detection algorithm, specifically that of the Hough circular transform, would be more consistent for the bulbs on the platform.

Another observation would be the importance of using adequate lighting for the detection component of the experiment. The samples had a set of LED lights used overhead to provide relatively consistent lighting throughout the setup, which is a requirement for a consistent machine vision output but some external light still reflected throughout the testing setup. It would be beneficial in future to ensure that the lighting only comes from a consistent source (i.e. the mentioned top-down LED light) and that the testing platform is covered in a light prohibiting shroud during machine vision testing.

3.4. Neural Network Investigation

Deeplab was used to provide comparable semantic segmentation to a subset of the various bulb images taken for testing. The Deeplab solution had been conducted as a comparison between its segmentation and the segmentation conducted in the numerical method described in section 3.1. Figure 3.19 shows a sample segmentation output using a pre-trained Deeplab model, namely one that had been derived from MobilenetV2 (Sandler et al., 2018), as the pre-trained network. It can be seen that the model interprets the bulbs as birds. This is because no bulb data sets had been trained on the model above and it had not been trained to detect bulb heads.

Figure 3.19.: Example output used with a pre-trained neural network on a sample bulb image. The outputs are seen as birds since the network had not been trained for bulbs.

In future work, it would be advisable to develop a model further using transfer learning to apply the bulb heads as valid targets to the pre-trained network, since the model detected the bulbs relatively adequately without the use of any prior understanding of what the bulb should look like.

It should be acknowledged that the hardware requirements for the CNN method are vastly higher than that of classical numerical shape analysis. CNN typically require a large GPU to process a large number of edge cases found in the CNN itself. The large GPU requirements mean that the hardware required on the mechanism would be more expensive and must be protected from dust damage as well. The GPU would also require a much larger power supply, a supply that the current mechanism cannot provide at this time. The limitations of the current mechanism should be acknowledged when investigating the optimal machine vision algorithm for the Automated Bulb Planter.

3.4.1. Summary

In conclusion, the 75 per cent success rate of detecting the bulbs was found to be a relatively successful output, taking into consideration all the constraints that could provide failure during detection. Many improvements could be made to optimise the detection of the bulb heads. The use of a machine vision system to detect and manipulate the bulbs for the Automate Bulb Planter was found to be promising within the manipulator's frame of reference. It should also be acknowledged that the manipulation system would be an iterative system, meaning that if a failure does occur during detection and manipulation, that the system would retry the same bulb until it gets manipulated from the bulbs platform itself.

4. Manipulation and End Effectors

The following chapter describes the analysis conducted by applying the vision system to a manipulation system that would mimic the intended design for the current automated bulb planter used by *Lilies by Blewden*. Further understanding of the bulbs overall characteristics and the assumptions made before manipulation should be acknowledged before discussing the validity of the manipulation testing conducted.

4.1. Bulb Characteristics

The following section describes the practical constraints that had to be considered for the automated component of the *ABP* and what would be needed to provide a working prototype on the mechanism itself. A proposal for a working concept would also be provided. *Lilies by Blewden* produce two lily variations on their farms, namely the traditional and oriental lily variations. Both of which have very differing bulb characteristics that needed to be considered for identification and manipulation. The oriental bulbs typically have a whiter head complexion than their traditional bulb counterparts, where the traditional bulbs typically have a brown coloring with a more pronounced clove structure. The oriental bulb heads are also typically smaller in diameter than the traditional bulbs.

Sizes for the bulbs vary in a range between 35mm and 55mm in diameter, while the mass differs from 30g up to 80g. The ease of damaging the bulbs was an important factor when evaluating the feasible manipulation methods available for the lily bulbs. Ingressive methods of manipulation would be impossible since it would ultimately destroy the bulbs before they are planted, while a mechanical gripper manipulation would require high precision due to the varying size for the bulbs, requiring a varied entry for the mechanical gripper

Another key component of the bulbs that needed to be considered in its manipulation, is the high permeability of the bulb head. This needed to be taken into account when considering vacuum manipulation as a valid approach since it would require a very high flow rate to account for the seepage present on the head itself.

4.2. Assumptions

The following assumptions were made on the overall structure of the process used for the automated manipulation of the bulbs. These assumptions were needed to determine an adequate scenario for the machine vision investigation. The bulbs would also be cleared of the majority of the peat present when they were initially stored in their respective crates. The storage would be done either manually as a pre-step before packing into the mentioned source or using an oscillating filtering mechanism that would prepare the bulbs before storage.

The bulb would be placed evenly spaced on a conveyor platform during detection and manipulation using an automated feed mechanism from a source. The feed conveyor would be static for the duration the detection and manipulation process. The conveyor would feed further bulbs from the source after the platform had been cleared of bulbs. The Notification of a clear platform would be provided by the detection system.

The bulbs would either be facing in North or South direction relative to their root structures on the conveyor feed. The simplified orientation is achieved with a mechanical manipulation where the bulbs get fed on the belt with a ramp feeding the bulbs to a wall that would forcibly rotate the bulbs to either a north or south facing direction. Prototyping was conducted to confirm the validity of this assumption.

The centre of the head of the bulb would be seen as an optimal target for an end effector to manipulate. The current manipulator uses a suction cup end effector that presses on the end of the bulb and applies suction to lift and manipulate the bulb itself. finding the head of the bulb is crucial for this manipulation process and it is assumed that an adequate head centroid be sent to the manipulator for its approach and lifting phases. Figure 4.1 shows an example of a suction cup end effector lifting a sample bulb head.

4.3. Manipulator Solution

The proposed solution for the lily bulb planting problem was to use a linear 3 Degree of Freedom gantry mounted on the mechanism, behind the augurs of the manipulator itself. The manipulator would approach the bulbs from a feed conveyor mounted on the mechanism. The approach co-ordinates would be determined using a camera detecting the heads of the bulbs using one of the standard machine vision solution mentioned in section 3.1. A suction cup end effector would lift a bulb head, move the head to one of the ten augured holes. The bulbs would be planted with the roots facing downwards by rotating the end effector 90 degrees in either the clockwise or anti-clockwise direction.

Figure 4.1.: Example of a bulb being lifted using a suction cup end effector. The head centroid is crucial for an optimal lifting procedure

The rotation direction would be determined from the machine vision algorithm detecting the root orientation present when the bulbs were placed statically on the conveyor platform.

Figure 4.2 shows a Computer Assisted Drawing of a prototype design for the 3 Degree of Freedom linear rail manipulator. The proposed idea had to be tested for its validity before the prototype could be purchased. The key components that had to be tested were the machine vision solution as well as the method of manipulating and planting the bulbs provided by *Lilies by Blewden*.

An industrial ABB arm was used as a substitute manipulator as a proof of concept. The ABB IRB120 arm, seen in Figure 4.4, was provided for testing by the University of Waikato's agriculture automation division and was used for testing the validity of the use of a 3-DOF manipulator with a suction end effector to manipulate the lily bulbs form a conveyor feed using a camera to identify the head positions for manipulation.

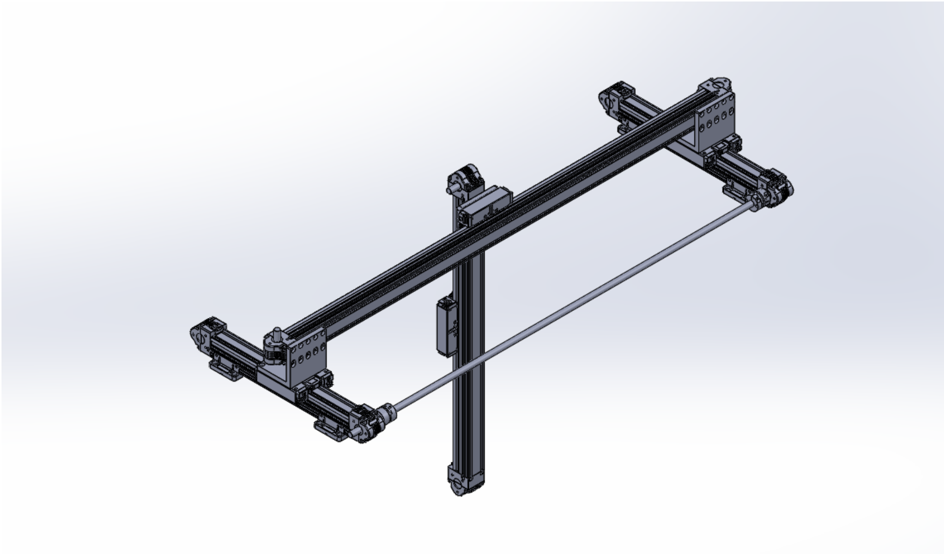

Figure 4.2.: CAD model of the proposed gantry prototype. The gantry would have a total of 4 linear rails moving the end effector in 3 linear directions of movement.

4.4. Results

4.4.1. Experimental Setup

The following section describes the experimental setup for the required investigation. The setup could be derived from the six phases shown in Figure 4.3, namely: Conveyor Feed, Bulb Identification, Co-ordinate Transfer, Manipulation and Iteration. Figure 4.4 presents the overall assembly for the experiment. The ABB arm would manipulate the bulbs on the conveyor belt using a suction cup as the end effector. The belt would be controlled based on the count of bulbs seen by the camera process, stopping at a set count of bulbs on the belt. The ABB arm would then systematically lift and manipulate the provided bulbs to the required sink.

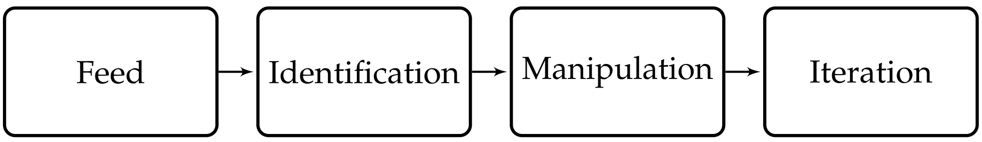

Figure 4.3.: Process Flow of the experimental setup required for a successful manipulation cycle

Bulbs are placed linearly with roots parallel to the linear direction, either front facing or rear facing. The orientation of the bulbs is based on the assumption that an adequate mechanical manipulation step had been conducted to orient the samples in either the north or south facing directions mentioned above.

A camera, 1.1m above the bulbs ground plane, takes an image of the bulbs, as seen in Figure 3.13a. The image is processed using OpenCV to determine the relative location of all the bulb heads displayed on the image. The direction of the roots are also evaluated based on the position of the bulb heads.

Given the relative co-ordinate and direction for all the bulbs have been processed, the relative pixel co-ordinates are converted to linear, arm co-ordinates using a linear transfer function, and then sent to the ABB arm as an ABB RAPID command relayed via a python script and a socket connection to the arms IRC5 controller.

The ABB universal arm directs itself to the nearest bulb head co-ordinate, manipulates it using a suction-based manipulator and rotates it so that root would be facing in the downwards direction. The arm moves the bulb towards the planting location and subsequently plants it using an external force to press it in place.

The ABB arm repeats the action until all bulbs on the provided image had been planted in their required locations. After all the bulbs were planted on the platform, the conveyor belt would feed an adequate amount of 4-6 bulbs toward the arms reach. The bulb count would be determined using a continuous machine vision stream, counting the bulbs on the platform every time it had attempted a planting sequence. The conveyor belt process would repeat itself when all the bulbs were planted on the platform. When all the bulbs had been planted visible on the platform, the conveyor would feed further bulbs until the infrared light sensor would be tripper again.

The success rate of the manipulator planting the bulbs would determine the overall feasibility of the manipulation system. This would determine whether the approach would be consistent enough to provide adequate results for the final prototype and whether the concept would be developed on further.

4.4.2. Manipulation Results

The final results found in the experiment were found to have an overall success rate of 41.38 per cent, as seen in Table 4.1. The table defines the success rate of each process, assuming that the previous process worked within its required degree of success so that the process is the only degree of error present. For example, the Engagement success rate was determined with test results that had a 100 per cent success rate during detection. The manipulation results were also divided into separate categories based on the most significant areas of possible failure when it comes to the manipulation of the bulbs from the conveyor belt to the sink. Raw data can be found in Appendix B.

From Table 4.1, it is clear to see that the cup engagement to the sample itself provided the most substantial amount of manipulation failure during testing.

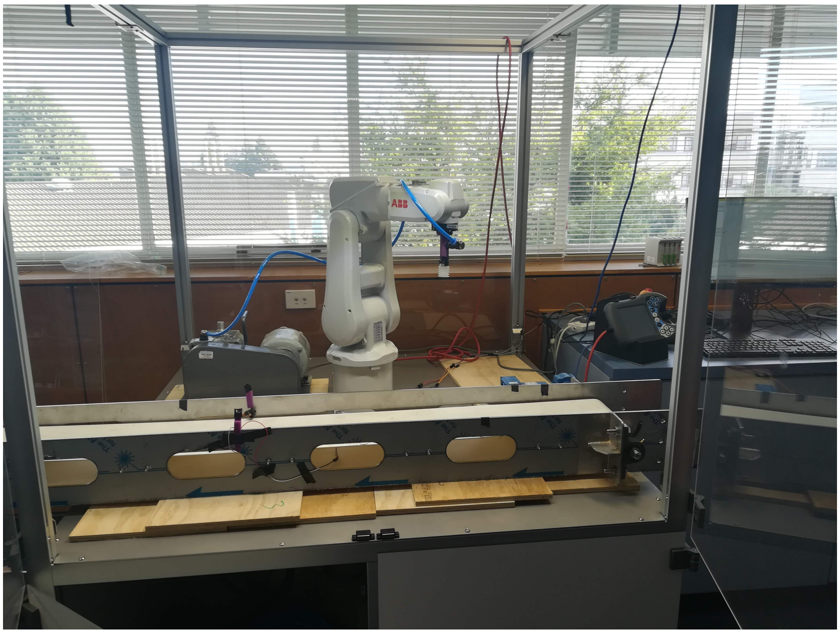

Figure 4.4.: Current ABB arm assembly used during prototyping. The suction end effector would lift and orient the bulbs present on the conveyor platform.

This failure makes sense since each bulb head would have a slightly different head structure even if the centroid had been detected.

Stage	Individual Success Rate (Percent)
Detection	74.26
Engagement	63.64
Manipulation	85.71
Planting	100.00

Table 4.1.: Success Rates for the varying stages of manipulation

4.4.3. Observations

The following observations were made with regards to the manipulators attempts to plant the bulb samples to a given sink.

The ABB arm was found to be difficult to handle using its built-in RAPID communication from the client. A socket connection had to be incorporated using Python and OpenCV as the interpreter between the data collected on the camera and the ABB manipulator since the dedicated ABB software was found to be very restrictive as to how it could be altered during experimentation. The alterations would be one of the many reasons as to why the ABB manipulator would not be a suitable solution for the final iteration for the automated bulb planter. Other reasons include the price, robustness in farming conditions as well as its speed.

It was found that the best region of engagement was at the centroid of the head itself and adequate regions were where the cup end effectors centroid was present within the bulb heads diameter. When the cups engagement region was at an edge scenario it was found the cups bellows would adjust to the steep angle of approach and encapsulate the top end of the bulb head.

It was observed that the suction gripper used to manipulate the bulbs were found to be more successful with samples that still had some water on the surface present, which makes sense since the water layer would prevent some seepage from occurring throughout the cloves of the bulbs themselves.

Another critical factor to adequate gripping was the structural integrity of individual cloves on the bulbs during the initial lifting sequence. Older bulbs (approx. week old) tend to have weaker cloves and could be torn off by the cup during the initial stages of lifting. Other issues include high vibration during manipulation for bulbs with weaker cloves, due to the oscillations on the clove itself. This oscillation could provide inconsistent planting if not considered.

The planting evaluation used for the results was not an adequate representation of the real world scenario. In the actual problem, the bulbs need to be pressed into the ground in order for it to fit snugly in the augered holes made by the current *ABP*. A 100 percent success rate was present due to the fact the bulb only needed to be oriented to the correct orientation and dropped to a sink prior to planting, rather than targeted into a small hole and pressed into place. The targeted planting and pressing must be considered for future work in order for an adequate manipulator process.

It should also be noted that the system was found to have an overall success rate of 50 per cent for a single attempt at manipulating the bulbs. The system was designed to provide multiple attempts on the same bulb to ensure that as many bulbs as possible get planted during the cycle. This repetition is done with an infrared sensor detecting the position of the final bulb on the belt. The infrared sensor would ensure that the manipulator would attempt to plant the same bulb at least twice before the bulb moves past the sensor and gets stored in a bulk sink for recycling into the system. It was found, after the second attempt of planting, that the overall success rate of the manipulator increases to 70 per cent. The likely reason for not obtaining close to 100 per cent is possibly due to the sample being an unusual shape for the camera to detect or possibly the manipulator not contacting the bulb properly due to weak cloves on the bulb, high amount of peat or the root structure obstructing an adequate contact region.

4.4.4. Further Prototyping

The final iteration of the *ABP* would need to involve the manipulation of bulbs with either north-south facing orientation. The bulbs would be manipulated from a conveyor feed using a linear 3-DOF gantry system, as seen in Figure 4.2. The gantry model shown is a prototype that had been proposed for assembly as an adequate testing rig for the ABP concept. The rig would be an adequate prototype to validate the proposed concept for the rough outdoors environment.

The relative position and orientation of each bulb on the belt would be detected using an image taken from an RGB camera positioned overhead of the conveyor belt. The heads and orientation of the bulbs would be calculated using an image processing algorithm specifically tuned for the environment and would consistently send accurate co-ordinate and orientation data to the manipulator. The manipulator would approach and manipulate each bulb individually towards the specified hole augured by the mechanism.

5. Conclusions and Future Work

In conclusion, the machine vision and manipulation techniques for lily bulb plantation was presented. The machine vision approach involved taking a top down image of the bulbs and identifying the head positions and what orientation they were facing relative to their root structures. This was achieved using various standard machine vision techniques like segmenting using global thresholding and identification of heads using the Hough circular transform. The investigated manipulation method involved applying the above mentioned vision system to a standard ABB IRB-120 universal manipulator with a three bellow suction gripper to pick up the detected bulbs and manipulate the bulbs in the orientation perceived by the vision system.

It was found that the machine vision algorithm provided a 75 per cent success rate when providing an optimal region of interest within the bulbs head. Improvements could be made to optimise the detection algorithm like improved lighting and better contrast between the bulbs colour gradient and that of the platform's background.

A 75 per cent success rate is a considerably successful result as the detection algorithm not only needed to detect the location of the bulbs, but the centroid of its head and also determine the approximate orientation relative to each samples individual root structure. Further work could be done to improve the algorithm and fine-tune the output provided.

The manipulation results showed that the engagement of the suction gripper was a significant component of failure during testing. The observed failure means that further improvements must be made before a successful end effector would be achieved. Improving suction rate or developing a specialized gripper for the specific amorphous bulbs would have to be investigated further before there is confirmation of a satisfactory solution for the Automated Lily Planter. Further development in the manipulator would also be conducted for validation.

5.1. Future Work

5.1.1. Vision Enhancements

The following section describes factors that could optimize the results in the future development of the machine vision algorithm. The main concern during the testing scenario was inconsistent lighting throughout as well as colour gradient similarities between the foreground bulbs and the background belt.

Ensuring consistent lighting throughout the detection phase of the process would be crucial to ensure optimal bulb detection and orientation identification. In future, an adequate method of limiting any external lighting would be necessary to provide the best results from the machine vision algorithm.

It was discovered that there was a considerable resemblance between the white background colour of the conveyor belt and the white oriental bulb heads used during testing. The colour similarities provided inconsistency during the numerical shape analysis since it likely discerned the background intensity of the belt to be similar to that of the head. Using a belt with a colour that contrasts the heads of both traditional and oriental bulbs would provide a better variation in intensity for the numerical algorithm to identify the required regions of interest.

An alternative method of detecting the bulbs would be to use a pre-trained segmentation neural network, mentioned in section 3.4, and retrain the model to detect and segment the lily bulb heads on the platform. The investigation into the performance of a neural network alternative could be promising as a pre-trained network had been found to provide relatively successful results, even without any retraining present in the network.

Given more time, the following would improve imaging and manipulation results for the current prototype. The enhancements would be expected to either provide a noticeable improvement in detection quality or provide a more consistent gripping and planting methods. Further work in terms of the feed and planting designs would also be discussed in the following section.

At the end of the experiment, issues were found with the pump used for testing, namely in overall suction rate and suction consistency. A possible upgrade to the pump may measurably improve the manipulation success rate present for the experiment. A pump with a higher suction rate that would adequately manipulate the bulb through the seeping cloves would help provide a more consistent manipulation. Addition of a proper grit filter would also be essential for repetitive testing throughout as well.

The primary end effector considered was a soft suction cup gripper with a large number of flexible bellows, since it had been proven a successful end effector for amorphous shapes (Hayashi et al., 2011). Other avenues for the end effector were not thoroughly investigated, and a more detailed end effector may improve consistency during manipulation.

5.1.2. Future Prototype Iterations

Before designing a final product for the *ABP*, further iteration is necessary to confirm other aspects needed for a successful process. Further development in the manipulator mechanism itself would be needed to substitute the ABB arm currently used since it is too expensive and would not be a robust enough solution for the current environment, which is a greenhouse with high quantities of peat and water present that could damage a universal arm such as the ABB IRB-120.

The following aspects should also be investigated and developed further before a final iteration could be installed to the Automated Bulb Planter. A magazine concept had been derived for the feed setup of the *ABP* to ensure an equal flow of bulbs onto the feed belt, where the bulbs would be manipulated. It was also proven that the bulbs would be manipulated mechanically so that all the bulb roots would either be facing in an upwards or downwards direction relative to the direction of movement on the belt. The pre-step bulb organisation would greatly assist in the manipulation process since the manipulator only needs to constrain its movement to a singular rotational degree of freedom in order to manipulate the bulb to the right direction for planting.

Further investigation into the feasibility of such a magazine design would be required before installation onto the *ABP*. The incorporation of it and the vision system would be crucial in determining the overall success of the automated component of the system.

An adequate planting mechanism must be developed to ensure a fully functional automated bulb planter. The bulbs must not only be placed in each individual hole, but must also be pressed into the hole deep enough for the roots to pierce the soil during planting, while not damaging the bulb head in the process.

Further development into an adequate planting mechanism must be conducted to ensure the Automated bulb planter works to the consistency required by *Lilies by Blewden*.

The currently proposed alternative to the ABB IRB-120 involves a 3-DOF gantry system mounted to the current auguring mechanism, with a rotating suction cup end effector lifting the bulbs from conveyor feed using a top-down camera as the bulb detector. Figure 5.1 shows a Computer Aided Model of the proposed prototype. Further work would ensure that this prototype is tested outside in a dusty and wet environment and that it would be a financially feasible alternative to planting the bulbs individually by hand.

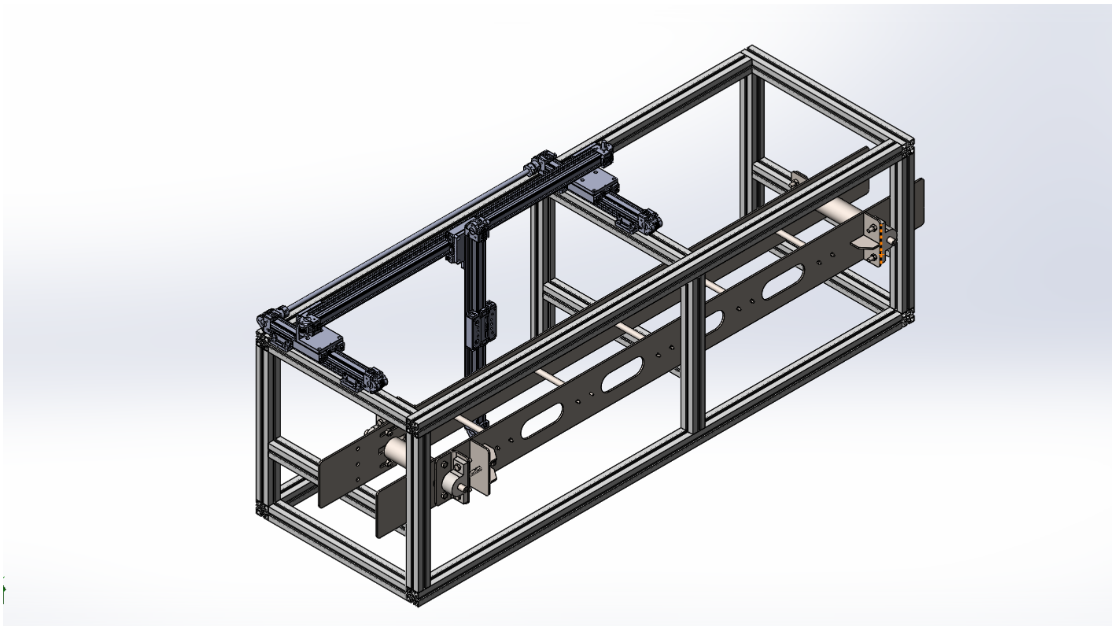

Figure 5.1.: CAD model of the proposed gantry prototype with the conveyor platform suspended using a frame for prototyping purposes. The conveyor would be used as the base platform used for the feed while the gantry system would lift and plant bulbs to the required holes.

Appendix

Appendix A.

Raw data

A.1. Success Validation Data

Region 1 <5mm	Region 2 5 - 10mm	Region 3 10 - 20mm
SUCCESS	SUCCESS	FAIL
SUCCESS	SUCCESS	SUCCESS
SUCCESS	SUCCESS	FAIL
SUCCESS	SUCCESS	FAIL
SUCCESS	SUCCESS	FAIL
SUCCESS	SUCCESS	SUCCESS
SUCCESS	FAIL	FAIL
SUCCESS	SUCCESS	FAIL
SUCCESS	SUCCESS	SUCCESS
SUCCESS	SUCCESS	SUCCESS
FAIL	SUCCESS	FAIL
SUCCESS	FAIL	FAIL
SUCCESS	SUCCESS	SUCCESS
FAIL	FAIL	FAIL
SUCCESS	SUCCESS	SUCCESS
SUCCESS	SUCCESS	FAIL
SUCCESS	SUCCESS	SUCCESS
SUCCESS	SUCCESS	FAIL
SUCCESS	SUCCESS	SUCCESS
SUCCESS	SUCCESS	FAIL
FAIL	FAIL	FAIL
SUCCESS	SUCCESS	FAIL
SUCCESS	SUCCESS	FAIL
SUCCESS	SUCCESS	SUCCESS
SUCCESS	SUCCESS	SUCCESS

A.2. Machine Vision Data

		Distance (mm)	Distance (Pixels)	
60.00	-22.00	43.15	63.91	BAD
-22.00	-1.00	14.87	22.02	GOOD
-7.00	-3.00	5.14	7.62	GOOD
8.00	-3.00	5.77	8.54	GOOD
-24.00	-14.00	18.76	27.78	BAD
49.00	-16.00	34.81	51.55	BAD
3.00	-8.00	5.77	8.54	GOOD
-16.00	-4.00	11.14	16.49	GOOD
-1.00	-3.00	2.14	3.16	GOOD
-6.00	6.00	5.73	8.49	GOOD
3.00	1.00	2.14	3.16	GOOD
-60.00	-5.00	40.66	60.21	BAD
-12.00	-4.00	8.54	12.65	GOOD
-21.00	-18.00	18.68	27.66	BAD
21.00	-1.00	14.20	21.02	GOOD
9.00	4.00	6.65	9.85	GOOD
8.00	-11.00	9.18	13.60	GOOD
-35.00	-16.00	25.99	38.48	BAD
-4.00	-6.00	4.87	7.21	GOOD
4.00	10.00	7.27	10.77	GOOD
11.00	0.00	7.43	11.00	GOOD
-11.00	-2.00	7.55	11.18	GOOD
2.00	-4.00	3.02	4.47	GOOD
6.00	2.00	4.27	6.32	GOOD
0.00	-12.00	8.10	12.00	GOOD
16.00	3.00	10.99	16.28	GOOD
-7.00	-6.00	6.23	9.22	GOOD
6.00	4.00	4.87	7.21	GOOD
1.00	-8.00	5.44	8.06	GOOD
17.00	7.00	12.41	18.38	GOOD
-3.00	-7.00	5.14	7.62	GOOD
7.00	3.00	5.14	7.62	GOOD
-51.00	0.00	34.44	51.00	BAD
49.00	45.00	44.92	66.53	BAD
-5.00	-8.00	6.37	9.43	GOOD
17.00	-9.00	12.99	19.24	GOOD
8.00	-1.00	5.44	8.06	GOOD
51.00	39.00	43.35	64.20	BAD
41.00	5.00	27.89	41.30	BAD
-15.00	2.00	10.22	15.13	GOOD
0.00	7.00	4.73	7.00	GOOD

Table A.2 continued from previous page

		Distance (mm)	Distance (Pixels)	
-32.00	19.00	25.13	37.22	BAD
4.00	3.00	3.38	5.00	GOOD
-8.00	-2.00	5.57	8.25	GOOD
14.00	3.00	9.67	14.32	GOOD
6.00	-1.00	4.11	6.08	GOOD
-7.00	1.00	4.77	7.07	GOOD
31.00	-6.00	21.32	31.58	BAD
-14.00	0.00	9.45	14.00	GOOD
-3.00	9.00	6.41	9.49	GOOD
7.00	6.00	6.23	9.22	GOOD
-10.00	-6.00	7.87	11.66	GOOD
288.00	-114.00	209.16	309.74	BAD
177.00	83.00	132.01	195.49	BAD
15.00	4.00	10.48	15.52	GOOD
14.00	1.00	9.48	14.04	GOOD
2.00	1.00	1.51	2.24	GOOD
4.00	0.00	2.70	4.00	GOOD
5.00	-4.00	4.32	6.40	GOOD
9.00	-5.00	6.95	10.30	GOOD
5.00	-2.00	3.64	5.39	GOOD
11.00	-12.00	10.99	16.28	GOOD
-10.00	-6.00	7.87	11.66	GOOD
65.00	-5.00	44.02	65.19	BAD
3.00	-8.00	5.77	8.54	GOOD
-54.00	19.00	38.66	57.25	BAD
37.00	-11.00	26.07	38.60	BAD
5.00	-6.00	5.27	7.81	GOOD
48.00	-13.00	33.58	49.73	BAD
-59.00	-44.00	49.70	73.60	BAD
3.00	7.00	5.14	7.62	GOOD
0.00	1.00	0.68	1.00	GOOD
4.00	6.00	4.87	7.21	GOOD
-57.00	9.00	38.97	57.71	BAD
8.00	2.00	5.57	8.25	GOOD
4.00	2.00	3.02	4.47	GOOD
15.00	1.00	10.15	15.03	GOOD
-52.00	29.00	40.20	59.54	BAD
22.00	8.00	15.81	23.41	BAD
13.00	1.00	8.80	13.04	GOOD
6.00	-7.00	6.23	9.22	GOOD
-13.00	5.00	9.41	13.93	GOOD
23.00	-14.00	18.18	26.93	BAD

Table A.2 continued from previous page

		Distance (mm)	Distance (Pixels)	
13.00	3.00	9.01	13.34	GOOD
-2.00	-10.00	6.89	10.20	GOOD
-14.00	2.00	9.55	14.14	GOOD
19.00	3.00	12.99	19.24	GOOD
14.00	6.00	10.29	15.23	GOOD
-15.00	-5.00	10.68	15.81	GOOD
86.00	-37.00	63.22	93.62	BAD
-10.00	1.00	6.79	10.05	GOOD
63.00	-16.00	43.89	65.00	BAD
21.00	2.00	14.24	21.10	GOOD
85.00	-31.00	61.09	90.48	BAD
-8.00	1.00	5.44	8.06	GOOD
-6.00	5.00	5.27	7.81	GOOD
12.00	9.00	10.13	15.00	GOOD
-5.00	8.00	6.37	9.43	GOOD
-12.00	-5.00	8.78	13.00	GOOD
-3.00	9.00	6.41	9.49	GOOD
172.00	-107.00	136.78	202.57	BAD
7.00	-2.00	4.92	7.28	GOOD
7.00	-14.00	10.57	15.65	GOOD
-10.00	8.00	8.65	12.81	GOOD
-6.00	-3.00	4.53	6.71	GOOD
12.00	11.00	10.99	16.28	GOOD
5.00	8.00	6.37	9.43	GOOD
-11.00	8.00	9.18	13.60	GOOD
-3.00	-6.00	4.53	6.71	GOOD
12.00	10.00	10.55	15.62	GOOD
-13.00	-3.00	9.01	13.34	GOOD
-7.00	-8.00	7.18	10.63	GOOD
77.00	14.00	52.85	78.26	BAD
13.00	3.00	9.01	13.34	GOOD
64.00	7.00	43.47	64.38	BAD
4.00	-2.00	3.02	4.47	GOOD
-14.00	4.00	9.83	14.56	GOOD
-1.00	-6.00	4.11	6.08	GOOD
-8.00	-11.00	9.18	13.60	GOOD
92.00	15.00	62.94	93.21	BAD
1.00	4.00	2.78	4.12	GOOD
23.00	-5.00	15.89	23.54	BAD
-10.00	1.00	6.79	10.05	GOOD
5.00	-5.00	4.77	7.07	GOOD
-23.00	38.00	29.99	44.42	BAD

Table A.2 continued from previous page

		Distance (mm)	Distance (Pixels)	
-43.00	6.00	29.32	43.42	BAD
9.00	0.00	6.08	9.00	GOOD
-54.00	-3.00	36.52	54.08	BAD
-2.00	-6.00	4.27	6.32	GOOD
-18.00	-4.00	12.45	18.44	GOOD
71.00	9.00	48.33	71.57	BAD
11.00	3.00	7.70	11.40	GOOD
3.00	1.00	2.14	3.16	GOOD
15.00	-6.00	10.91	16.16	GOOD
13.00	-2.00	8.88	13.15	GOOD
-4.00	-8.00	6.04	8.94	GOOD

A.3. Manipulation Data

Detection	Engagement	Manipulation	Planting
SUCCESS	SUCCESS	SUCCESS	SUCCESS
SUCCESS	SUCCESS	SUCCESS	SUCCESS
SUCCESS	FAIL	RECUR FAIL	RECUR FAIL
FAIL	RECUR FAIL	RECUR FAIL	RECUR FAIL
SUCCESS	FAIL	RECUR FAIL	RECUR FAIL
SUCCESS	SUCCESS	SUCCESS	SUCCESS
SUCCESS	FAIL	RECUR FAIL	RECUR FAIL
FAIL	RECUR FAIL	RECUR FAIL	RECUR FAIL
FAIL	RECUR FAIL	RECUR FAIL	RECUR FAIL
SUCCESS	FAIL	RECUR FAIL	RECUR FAIL
SUCCESS	SUCCESS	SUCCESS	SUCCESS
SUCCESS	SUCCESS	FAIL	RECUR FAIL
SUCCESS	SUCCESS	SUCCESS	SUCCESS
SUCCESS	FAIL	RECUR FAIL	RECUR FAIL
SUCCESS	SUCCESS	SUCCESS	SUCCESS
SUCCESS	FAIL	RECUR FAIL	RECUR FAIL
FAIL	RECUR FAIL	RECUR FAIL	RECUR FAIL
SUCCESS	SUCCESS	SUCCESS	SUCCESS
SUCCESS	SUCCESS	SUCCESS	SUCCESS
FAIL	RECUR FAIL	RECUR FAIL	RECUR FAIL
FAIL	RECUR FAIL	RECUR FAIL	RECUR FAIL
SUCCESS	SUCCESS	SUCCESS	SUCCESS
SUCCESS	SUCCESS	SUCCESS	SUCCESS
SUCCESS	FAIL	RECUR FAIL	RECUR FAIL
SUCCESS	SUCCESS	SUCCESS	SUCCESS
FAIL	RECUR FAIL	RECUR FAIL	RECUR FAIL

Table A.3 continued from previous page

Detection	Engagement	Manipulation	Planting
SUCCESS	FAIL	RECUR FAIL	RECUR FAIL
SUCCESS	SUCCESS	SUCCESS	SUCCESS
SUCCESS	SUCCESS	FAIL	RECUR FAIL

Bibliography

Andrew, Alex M. (2009). “Visual Servoing: Real-Time Control Of Robot Manipulators Based On Visual Sensory Feedback, edited by Koichi Hashimoto, Series in Robotics and Automated Systems vol. 1, World Scientific Singapore 1993, ISBN 981-02-1364-6, Hardcover, vii + 363 pp. (£56.00)”. In: *Robotica* 14.5, pp. 585–586. ISSN: 0263-5747. DOI: 10.1017/S0263574700020099. URL: https://www.cambridge.org/core/article/visual-servoing-realtime-control-of-robot-manipulators-based-on-visual-sensory-feedback-edited-by-koichi-hashimoto-series-in-robotics-and-automated-systems-vol-1-world-scientific-singapore-1993-isbn-9810213646-hardcover-vii-363-pp-5600/CC6515C01AD18087CDA2FAF81310AE72.

Ashton, Kevin et al. (2009). “That ‘internet of things’ thing”. In: *RFID journal* 22.7, pp. 97–114 (cit. on p. 1).

Azizpanah, Amir et al. (2015). “Precision spray modeling using image processing and artificial neural network”. In: *Agricultural Engineering International: CIGR Journal* 17.2, pp. 65–74. ISSN: 16821130. URL: http://search.ebscohost.com/login.aspx?direct=true&db=a9h&AN=108385463&site=ehost-live.

Bac, C. Wouter et al. (2014). “Harvesting Robots for High-value Crops: State-of-the-art Review and Challenges Ahead”. In: *Journal of Field Robotics* 31.6, pp. 888–911. ISSN: 1556-4967. DOI: 10.1002/rob.21525. URL: http:https://doi.org/10.1002/rob.21525.

Barnett, Josh (2018). “Prismatic axis, differential-drive robotic kiwifruit harvester for reduced cycle time”. Masters. PhD thesis. Hamilton, New Zealand. URL: https://hdl.handle.net/10289/12444 (cit. on p. 1).

Blanes, C. et al. (2011). “Review. Technologies for robot grippers in pick and place operations for fresh fruits and vegetables”. In: *Spanish Journal of Agricultural Research* 9.4, p. 12. ISSN: 2171-9292. DOI: 10.5424/sjar/20110904-501-10. URL: http://revistas.inia.es/index.php/sjar/article/view/2437 (cit. on pp. 11, 12).

Brooks, R. (1986). “A robust layered control system for a mobile robot”. In: *IEEE Journal on Robotics and Automation* 2.1, pp. 14–23. ISSN: 0882-4967. DOI: 10.1109/JRA.1986.1087032 (cit. on p. 1).

Budynas, Richard G., J. Keith Nisbett, and Joseph Edward Shigley (2015). *Shigley’s mechanical engineering design*. ISBN: 9780073398204 0073398209 9789814595285 9814595284 9780077172282 0077172280.

Chen, Liang-Chieh et al. (2018). "Encoder-Decoder with Atrous Separable Convolution for Semantic Image Segmentation". In: *ECCV* (cit. on p. 10).

Costa, Luciano da Fontoura Da and Jr. Roberto Marcondes Cesar (2000a). *Shape Analysis and Classification: Theory and Practice*. CRC Press, Inc., p. 680. ISBN: 0849334934 (cit. on p. 14).

Costa, Luciano da Fontoura Da and Jr. Roberto Marcondes Cesar (2000b). "Shape Analysis and Classification: Theory and Practice". In: CRC Press, Inc. Chap. Shape Aquisition and Processing, pp. 197–264. ISBN: 0849334934 (cit. on p. 8).

Dash, Sonali and Uma Ranjan Jena (2017). "Multi-resolution Laws' Masks based texture classification". In: *Journal of Applied Research and Technology* 15.6, pp. 571–582. ISSN: 1665-6423. DOI: `https://doi.org/10.1016/j.jart.2017.07.005`. URL: `http://www.sciencedirect.com/science/article/pii/S1665642317301049`.

Foglia Mario, M. and Giulio Reina (2006). "Agricultural robot for radicchio harvesting". In: *Journal of Field Robotics* 23.6-7, pp. 363–377. ISSN: 1556-4959. DOI: `10.1002/rob.20131`. URL: `https://doi.org/10.1002/rob.20131` (cit. on p. 13).

Garcia-Lamont, Farid et al. (2018). "Segmentation of images by color features: A survey". In: *Neurocomputing* 292, pp. 1–27. ISSN: 0925-2312. DOI: `https://doi.org/10.1016/j.neucom.2018.01.091`. URL: `http://www.sciencedirect.com/science/article/pii/S0925231218302364`.

Gonzalez, Rafael C. and Richard E. Woods (2001). *Digital Image Processing*. 2nd. Boston, MA, USA: Addison-Wesley Longman Publishing Co., Inc. ISBN: 0201180758 (cit. on p. 14).

Gonzalez, Rafael C., Richard E. Woods, and Steven L. Eddins (2003). *Digital Image Processing Using MATLAB*. Prentice-Hall, Inc. ISBN: 0130085197 (cit. on pp. 7, 14).

Goodfellow, Ian, Yoshua Bengio, and Aaron Courville (2016). *Deep Learning*. `http://www.deeplearningbook.org`. MIT Press (cit. on p. 9).

Günther, Hans-Otto and Kap Hwan Kim (2005). *Container terminals and automated transport systems*. Springer (cit. on p. 1).

Han, L. et al. (2018). "DEVELOPMENT OF A MULTI-TASK ROBOTIC TRANSPLANTING WORKCELL FOR GREENHOUSE SEEDLINGS". In: *Applied Engineering in Agriculture* 34.2, pp. 335–342. ISSN: 0883-8542. DOI: `10.13031/aea.12462`. URL: `%3CGo%20to%20ISI%3E://WOS:000430507300009` (cit. on p. 12).

Hayashi, Shigehiko et al. (2011). "Gentle handling of strawberries using a suction device". In: *Biosystems Engineering* 109.4, pp. 348–356. ISSN: 1537-5110. DOI: `https://doi.org/10.1016/j.biosystemseng.2011.04.014`. URL: `http://www.sciencedirect.com/science/article/pii/S153751101100078X` (cit. on pp. 11, 12, 40).

Hibbeler, Russell C. and Kai Beng Yap (2018). *Mechanics of materials*. Harlow: Pearson. ISBN: 1292178205 9781292178202.

Hockstein, N. G. et al. (2007). "A history of robots: from science fiction to surgical robotics". In: *Journal of Robotic Surgery* 1.2, pp. 113–118. ISSN: 1863-2491. DOI: 10.1007/s11701-007-0021-2. URL: https://doi.org/10.1007/s11701-007-0021-2 (cit. on p. 1).

Hoefling, M. et al. (2015). "Enabling resilient smart grid communication over the information-centric C-DAX middleware". In: *2015 International Conference and Workshops on Networked Systems (NetSys)*, pp. 1–8. DOI: 10.1109/NetSys.2015.7089080 (cit. on p. 1).

Horn, Berthold, Berthold Klaus, and Paul Horn (1986). *Robot vision*. MIT press (cit. on p. 1).

Kumar, Pankaj et al. (2014). "Root phenotyping by root tip detection and classification through statistical learning". In: *Plant and Soil* 380.1, pp. 193–209. ISSN: 1573-5036. DOI: 10.1007/s11104-014-2071-3. URL: https://doi.org/10.1007/s11104-014-2071-3 (cit. on p. 6).

Liu, Chenxi et al. (2019). "Auto-DeepLab: Hierarchical Neural Architecture Search for Semantic Image Segmentation". In: *CVPR* (cit. on p. 10).

Liu, Songtao et al. (2012). "Optimal Design of a 4-DOF SCARA Type Parallel Robot Using Dynamic Performance Indices and Angular Constraints". In: *Journal of Mechanisms and Robotics* 4.3. ISSN: 1942-4302. DOI: 10.1115/1.4006743. URL: http://dx.doi.org/10.1115/1.4006743.

MathWorks (2019). *MATLAB Hough transform formulation*. URL: https://www.mathworks.com/help/images/ref/hough.html (visited on 05/28/2019).

McGuinness, Benjamin John (2018). "Investigation of a 'Field Factory' to Harvest and Grade Tree Stock in a Forestry Nursery". Doctoral. PhD thesis. Hamilton, New Zealand. URL: https://hdl.handle.net/10289/12245 (cit. on p. 1).

Michael Nielsen (2018). *DeepLearning*. [Online; accessed May 30, 2019]. URL: http://neuralnetworksanddeeplearning.com/chap6.html (cit. on p. 10).

Mizushima, Akira and Renfu Lu (2013). "An image segmentation method for apple sorting and grading using support vector machine and Otsu's method". In: *Computers and Electronics in Agriculture* 94, pp. 29–37. ISSN: 0168-1699. DOI: https://doi.org/10.1016/j.compag.2013.02.009. URL: http://www.sciencedirect.com/science/article/pii/S0168169913000483 (cit. on p. 6).

Mohammadi Baneh, Nesar, Hosein Navid, and Jalal Kafashan (2018). "Mechatronic components in apple sorting machines with computer vision". In: *Journal of Food Measurement and Characterization* 12.2, pp. 1135–1155. ISSN: 2193-4134. DOI: 10.1007/s11694-018-9728-1. URL: https://doi.org/10.1007/s11694-018-9728-1.

Nagasaka, Yoshisada et al. (2004). "Autonomous guidance for rice transplanting using global positioning and gyroscopes". In: *Computers and Electronics in Agriculture* 43.3, pp. 223–234. ISSN: 0168-1699. DOI: https://doi.org/10.1016/j.compag.2004.01.005. URL: http://www.sciencedirect.com/science/article/pii/S0168169904000304.

Nasrabadi, Nasser M. "Pattern Recognition and Machine Learning". In: vol. 16. SPIE.

Nausheen, Nazma et al. (2018). "A FPGA based implementation of Sobel edge detection". In: *Microprocessors and Microsystems* 56, pp. 84–91. ISSN: 0141-9331. DOI: https://doi.org/10.1016/j.micpro.2017.10.011. URL: http://www.sciencedirect.com/science/article/pii/S0141933116302289.

Noguchi, N et al. (1998). "Vehicle automation system based on multi-sensor integration". In: *ASAE paper* 983111 (cit. on p. 1).

Otsu, N. (1979). "A Threshold Selection Method from Gray-Level Histograms". In: *IEEE Transactions on Systems, Man, and Cybernetics* 9.1, pp. 62–66. ISSN: 0018-9472. DOI: 10.1109/TSMC.1979.4310076 (cit. on p. 16).

Pal, Nikhil R. and Sankar K. Pal (1993). "A review on image segmentation techniques". In: *Pattern Recognition* 26.9, pp. 1277–1294. ISSN: 0031-3203. DOI: https://doi.org/10.1016/0031-3203(93)90135-J. URL: http://www.sciencedirect.com/science/article/pii/003132039390135J.

Parker, J. R. (1996). *Algorithms for Image Processing and Computer Vision*. John Wiley
amp; Sons, Inc., p. 417. ISBN: 0471140562 (cit. on pp. 7, 9, 14).

Rafiq, Aasima, A. Makroo Hilal, and K. Hazarika Manuj (2015). "Artificial Neural Network-Based Image Analysis for Evaluation of Quality Attributes of Agricultural Produce". In: *Journal of Food Processing and Preservation* 40.5, pp. 1010–1019. ISSN: 0145-8892. DOI: 10.1111/jfpp.12681. URL: https://doi.org/10.1111/jfpp.12681.

Razmjooy, Navid, B. Somayeh Mousavi, and F. Soleymani (2012). "A real-time mathematical computer method for potato inspection using machine vision". In: *Computers Mathematics with Applications* 63.1, pp. 268–279. ISSN: 0898-1221. DOI: https://doi.org/10.1016/j.camwa.2011.11.019. URL: http://www.sciencedirect.com/science/article/pii/S0898122111009850 (cit. on p. 7).

Remondino, Fabio and David Stoppa (2013). *TOF Range-Imaging Cameras*. Springer Publishing Company, Incorporated, p. 245. ISBN: 9783642275227.

Roth, B. (1986). "Scientific fundamentals of robotics 4: Real-time dynamics of manipulation robots". In: *IEEE Control Systems Magazine* 6.6, pp. 19–20. ISSN: 0272-1708. DOI: 10.1109/MCS.1986.1105167.

Rowe, Philip (2015). "Optical Techniques for Fruit Firmness Assessment". Doctoral. PhD thesis. Hamilton, New Zealand. URL: https://hdl.handle.net/10289/9208 (cit. on p. 1).

Sabanci, Kadir, Ahmet Kayabasi, and Abdurrahim Toktas (2016). "Computer vision-based method for classification of wheat grains using artificial neural network". In: *Journal of the Science of Food and Agriculture* 97.8, pp. 2588–2593. ISSN: 0022-5142. DOI: 10.1002/jsfa.8080. URL: https://doi.org/10.1002/jsfa.8080 (cit. on p. 5).

Sandler, Mark et al. (2018). "MobileNetV2: Inverted Residuals and Linear Bottlenecks". In: *CVPR* (cit. on pp. 10, 28).

Singh, Veerendra and R. Mishra (2006). "Developing a machine vision system for spangle classification using image processing and artificial neural network". In: *Surface and Coatings Technology* 201.6, pp. 2813–2817. ISSN: 0257-8972. DOI: https://doi.org/10.1016/j.surfcoat.2006.05.031. URL: http://www.sciencedirect.com/science/article/pii/S0257897206004506.

Solomon, Chris and Toby Breckon (2011). *Fundamentals of Digital Image Processing: A Practical Approach with Examples in Matlab*. Wiley Publishing, p. 344. ISBN: 9780470844731 (cit. on p. 14).

Sun, Da-Wen (2000). "Inspecting pizza topping percentage and distribution by a computer vision method". In: *Journal of Food Engineering* 44.4, pp. 245–249. ISSN: 0260-8774. DOI: https://doi.org/10.1016/S0260-8774(00)00024-8. URL: http://www.sciencedirect.com/science/article/pii/S0260877400000248 (cit. on p. 5).

Tao, Dacheng, Dianhui Wang, and Fionn Murtagh (2013). "Machine learning in intelligent image processing". In: *Signal Processing* 93.6, pp. 1399–1400. ISSN: 0165-1684. DOI: https://doi.org/10.1016/j.sigpro.2013.02.004. URL: http://www.sciencedirect.com/science/article/pii/S0165168413000479.

Töreyin, B. Uğur et al. (2006). "Computer vision based method for real-time fire and flame detection". In: *Pattern Recognition Letters* 27.1, pp. 49–58. ISSN: 0167-8655. DOI: https://doi.org/10.1016/j.patrec.2005.06.015. URL: http://www.sciencedirect.com/science/article/pii/S0167865505001819 (cit. on p. 6).

Vukobratović, Miomir (1985). *Real-time dynamics of manipulation robots*. Berlin New York: Berlin New York : Springer-Verlag.

Yasmin, Jaseema and Mohamed Sathik (2015). "An Improved Iterative Segmentation Algorithm using Canny Edge Detector for Skin Lesion Border Detection". In: *International Arab Journal of Information Technology (IAJIT)* 12.4, pp. 325–332. ISSN: 16833198. URL: http://search.ebscohost.com/login.aspx?direct=true&db=iih&AN=108383556&site=ehost-live.

Yihong Gong, Wei Xu (2007). *Machine learning for multimedia content analysis*.

Zheng, Xiaoqiang (2016). *TensorFlow: A System for Large-Scale Machine Learning*. Report.